

RESEARCH PAPER

 OPEN ACCESS 

2-Arylquinolines as novel anticancer agents with dual EGFR/FAK kinase inhibitory activity: synthesis, biological evaluation, and molecular modelling insights

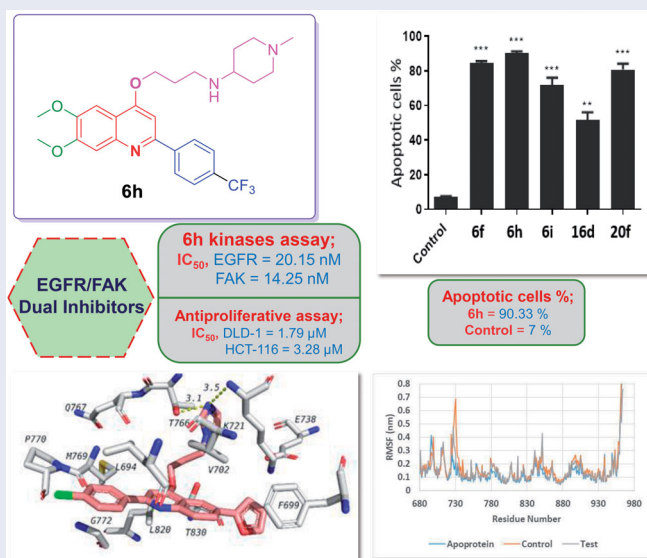
Mostafa M. Elbadawi^{a,b}, Wagdy M. Eldehna^b, Amer Ali Abd El-Hafeez^{c,d}, Warda R. Somaa^e, Amgad Albohy^f, Sara T. Al-Rashood^g, Keli K. Agama^h, Eslam B. Elkaeedⁱ, Pradipta Ghosh^{d,j,k,l}, Yves Pommier^h and Manabu Abe^a

^aDepartment of Chemistry, Graduate School of Science, Hiroshima University, Hiroshima, Japan; ^bDepartment of Pharmaceutical Chemistry, Faculty of Pharmacy, Kafrelsheikh University, Kafrelsheikh, Egypt; ^cPharmacology and Experimental Oncology Unit, Cancer Biology Department, National Cancer Institute, Cairo University, Cairo, Egypt; ^dDepartment of Cellular and Molecular Medicine, University of California San Diego, La Jolla, CA, USA; ^eFaculty of Pharmacy, Kafrelsheikh University, Kafrelsheikh, Egypt; ^fDepartment of Pharmaceutical Chemistry, Faculty of Pharmacy, The British University in Egypt (BUE), Cairo, Egypt; ^gDepartment of Pharmaceutical Chemistry, College of Pharmacy, King Saud University, Riyadh, Saudi Arabia; ^hDevelopmental Therapeutics Branch, Laboratory of Molecular Pharmacology, Center for Cancer Research, National Cancer Institute, NIH, Bethesda, MD, USA; ⁱDepartment of Pharmaceutical Sciences, College of Pharmacy, AlMaarefa University, Riyadh, Saudi Arabia; ^jDepartment of Medicine, University of California San Diego, La Jolla, CA, USA; ^kMoore's Comprehensive Cancer Center, University of California San Diego, La Jolla, CA, USA; ^lVeterans Affairs Medical Center, La Jolla, CA, USA

ABSTRACT

In this study, different assortments of 2-arylquinolines and 2,6-diarylquinolines have been developed. Recently, we have developed a new series of 6,7-dimethoxy-4-alkoxy-2-arylquinolines as Topoisomerase I (TOP1) inhibitors with potent anticancer activity. Utilising the SAR outputs from this study, we tried to enhance anticancer and TOP1 inhibitory activities. Though target quinolines demonstrated potent antiproliferative effect, specifically against colorectal cancer DLD-1 and HCT-116, they showed weak TOP1 inhibition which may be attributable to their non-coplanarity. Thereafter, screening against kinase panel revealed their dual inhibitory activity against EGFR and FAK. Quinolines **6f**, **6h**, **6i**, and **20f** were the most potent EGFR inhibitors (IC_{50} s = 25.39, 20.15, 22.36, and 24.81 nM, respectively). Meanwhile, quinolines **6f**, **6h**, **6i**, **16d**, and **20f** exerted the best FAK inhibition (IC_{50} s = 22.68, 14.25, 18.36, 17.36, and 15.36 nM, respectively). Finally, molecular modelling was employed to justify the promising EGFR/FAK inhibition. The study outcomes afforded the first reported quinolines with potent EGFR/FAK dual inhibition.

GRAPHICAL ABSTRACT




ARTICLE HISTORY

Received 12 November 2021
Revised 29 November 2021
Accepted 1 December 2021

KEYWORDS

Quinoline; anticancer; EGFR inhibitors; FAK inhibitors; molecular dynamics

CONTACT Mostafa M. Elbadawi  mostafa_elbadawi@pharm.kfs.edu.eg  Department of Chemistry, Graduate School of Science, Hiroshima University, 1-3-1 Kagamiyama, Higashi-Hiroshima, Hiroshima, 739-8526, Japan; Wagdy M. Eldehna  wagdy2000@gmail.com  Department of Pharmaceutical Chemistry, Faculty of Pharmacy, Kafrelsheikh University, Kafrelsheikh, 33516, Egypt; Manabu Abe  mabe@hiroshima-u.ac.jp  Department of Chemistry, Graduate School of Science, Hiroshima University, 1-3-1 Kagamiyama, Higashi-Hiroshima, Hiroshima, 739-8526, Japan

 Supplemental data for this article can be accessed [here](#).

© 2021 The Author(s). Published by Informa UK Limited, trading as Taylor & Francis Group.

This is an Open Access article distributed under the terms of the Creative Commons Attribution License (<http://creativecommons.org/licenses/by/4.0/>), which permits unrestricted use, distribution, and reproduction in any medium, provided the original work is properly cited.

1. Introduction

Cancer is a major health obstacle in the world threatening the life of millions of people annually^{1,2}. The universal burden of cancer has been expected to rise to 21.6 million in 2023 compared to 14.1 million in 2012 and was predicted to increase to 28.4 million in 2040 with 47% increment relative to 2020³⁻⁵. In 2020, 19.3 million new cancer cases have been diagnosed and 10 million cancer patients passed away. As established by WHO in 2019, cancer was estimated to be the first or second dominant cause of death for the ages <70 years in 112 countries, while it was projected to be the third or fourth death cause in 23 countries. In general, the incidence and mortality of cancer are growing rapidly worldwide^{4,6}. Subsequently, enormous attempts have been implemented to develop potent anticancer drugs through investigations of diverse scaffolds against numerous potential chemotherapeutic targets⁷⁻⁹.

Epidermal growth factor receptor (EGFR) is a member of tyrosine kinase family in which the endogenous ligand binds to the extracellular domain leading to conformational changes and dimerisation of EGFR resulting in its activation which subsequently stimulates its intrinsic intracellular protein-tyrosine kinase activity¹⁰. EGFR is over-expressed in many solid tumours and is related to cancer cell proliferation, angiogenesis and metastasis, so it has a critical role in cancer growth. Therefore, EGFR has been validated as an efficient target for anticancer drug discovery. In the

last two decades, different 4-anilinoquinazoline-based EGFR inhibitors, such as Gefitinib, Erlotinib, Afatinib, and Dacomitinib (Figure 1), have been FDA-approved for clinical use in treatment of non-small cell lung cancer^{11,12}.

Focal adhesion kinase (FAK) is a cytoplasmic non-receptor tyrosine kinase involved in signal transductions from cell adhesions to regulate different biological cell functions including survival and cell migration^{13,14}. Also, it is activated and overexpressed in diverse cancer types controlling cancer proliferation, survival and metastasis. Thus, FAK has been identified as a promising drug-gable target for targeted cancer therapy. Currently, several FAK inhibitors, such as 2,4-diaminopyridine derivative GSK2256098 and 2,4-diaminopyrimidine derivative Defactinib (Figure 1), are currently being evaluated in clinical trials for cancer treatment, in addition to the 2,4-diaminopyrimidine derivative TAE-226 (Figure 1) which displayed potent antitumor impact in different cancer types *in vivo* and *in vitro* and usually used as a reference drug^{7,15,16}. Noteworthy, it was established that the most affected colorectal cancer expressed high levels of EGFR and FAK that particularly correlated with tumour angiogenesis, cancer aggressiveness and poor prognosis^{17,18}.

Thus, dual EGFR/FAK inhibition mechanism is an efficient strategy to fight cancer that could be attributed to a non-overlapping downstream signalling/inhibition^{19,20}. For example, the kinase inhibitor APG-2449 (Figure 1) was reported to improve the antitumor effect of Ibrutinib *via* EGFR/FAK inhibition mechanism in

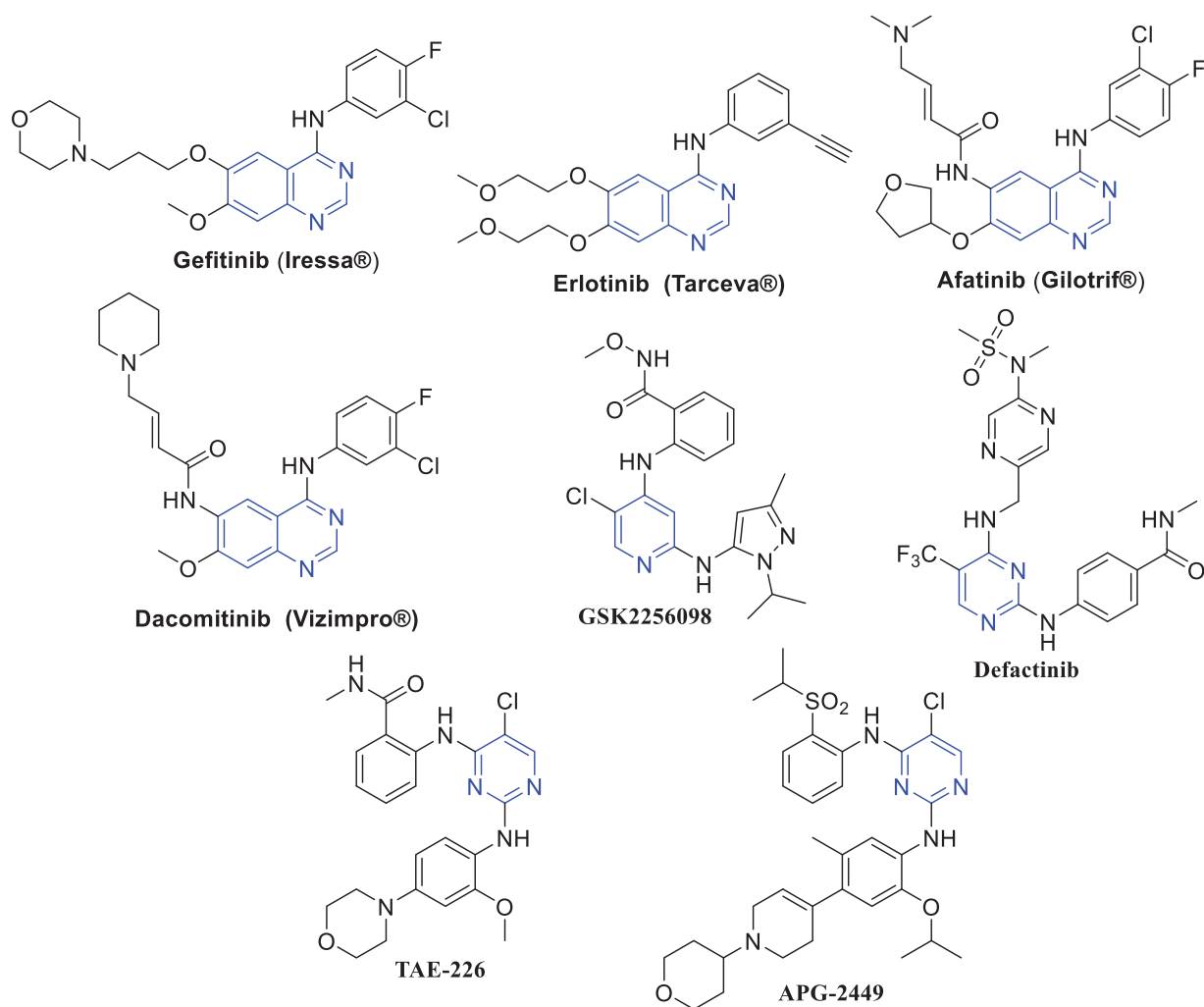


Figure 1. Some reported EGFR and FAK inhibitors.

oesophageal squamous cell carcinoma¹⁹. Also, combined EGFR/FAK inhibition caused higher radiosensitization than either approach alone²¹. Interestingly, few studies have succeeded to develop dual EGFR/FAK small molecule inhibitors. In 2020, Ai et al. has exploited a fragment-based drug design approach to identify novel series of 2,4-diaminopyrimidines as potent dual EGFR/FAK inhibitors with good *in vitro* and *in vivo* antitumor effects²⁰.

Quinoline is an outstanding planar heterocyclic motif playing a distinctive role in anticancer drug discovery. So far, assortments of quinoline-based small molecules have been developed and investigated against numerous biological targets for cancer treatment displaying exquisite outcomes^{22–25}. It is worth stressing that plenty of quinoline derivatives provoked their anticancer impact through different mechanisms of action, such as inhibition of DNA repair, tubulin polymerisation, and inhibition of various enzymes implicated in critical cancer cell proliferation prominently kinases enzymes (EGFR, VEGFR, pim-1 kinase, c-Met factor, and PI3K) which stood out as one of the most significant targets implemented in cancer therapy due to their functions in cellular signal transduction^{26–30}. Of special interest, Pelitinib (EKB-569, Figure 2) is a 4-anilinoquinoline derivative which is a potent irreversible inhibitor of EGFR in the clinical trials as an anticancer candidate²⁴. In addition, several 4-aminoquinoline derivatives, such as compounds I–III (Figure 2), were reported as promising EGFR inhibitors endowed with effective anticancer activities. Accordingly, quinoline stands out as a significant privileged scaffold in anticancer drug discovery to develop many efficient kinases inhibitors^{24,31–35}.

Recently, we have developed a new series of 6,7-dimethoxy-4-alkoxy-2-arylquinolines as potential Topoisomerase I (TOP1) inhibitors³⁶. The TOP1-mediated DNA cleavage assay was utilised to assess the ability of the reported compounds to stabilise TOP1-DNA cleavage complexes (TOP1ccs). The assay outcomes revealed a moderate TOP1 inhibitory activity of compounds IVa,b (Figure 2). Interestingly, the developed quinolines showed outstanding anti-proliferative profile upon evaluation at the Developmental Therapeutics Program (DTP) of the NCI-USA. Noteworthy, the weightiness of incorporation of *p*-substituted phenyl at C-2, as

well as propyl linker at C-4 of the quinoline scaffold, was highlighted by the SAR study.

As a continuation for our previous study³⁶ novel five sets of 4-propoxy-2-arylquinolines (**6a–o**, **8a,b**, **10a,b**, **12a–d**, **16a–d**), and 4-propoxy-2,6-diarylquinolines (**20a–f**) are herein designed and synthesised, exploiting the deduced SARs from the previous study, with the aim to afford more potent anticancer TOP1 inhibitors (Figure 2). Different structural modification strategies were adopted seeking to enhance both anticancer and TOP1 inhibitory activities of the lead compounds IVa,b (Figure 3).

First, diverse secondary alicyclic and aromatic amines, in addition to different primary amines were appended to the propyl linker to illuminate the influence of these moieties on the activity. Also, we introduced the electron donating methyl group as well as electron withdrawing Cl and CF₃ for more elucidation of the electronic impact of *p*-substituent of the 2-phenyl. Likewise, the heterocycles: 2-furyl and 2-thienyl were appended to *para* position of the C2-phenyl moiety to explore their electronic and size impact on the desired activity. Afterward, the 6,7-dimethoxy groups were removed in some synthesised analogs to confirm their significance. Moreover, the ring system was extended *via* fusion of the quinoline motif with 1,3-dioxolane in attempt to enhance the planar structure requisite for DNA intercalation which may potentiate both anticancer and TOP1 poisoning effects. Finally, a structural extension approach was utilised *via* grafting the HBA-bearing 2-furyl and 4-methoxyphenyl moieties at C6 of quinoline scaffold, hoping to enhance the hydrophobic interactions (Figure 3). The designed 4-propoxy-2-arylquinolines were prepared employing different synthetic procedures, and then investigated for their anticancer and TOP1 inhibitory activities.

Although the target quinolines demonstrated potent antiproliferative effect against different cancer cell lines, they showed no or weak TOP1 poisoning influence. Accordingly, the promising anticancer activity prompted us to search for the plausible molecular mechanism for herein reported quinolines.

The diverse well-reported kinase inhibitory activities of quinoline-based small molecules, as mentioned above, motivated us to explore the potential inhibitory activity of target 4-propoxy-2-

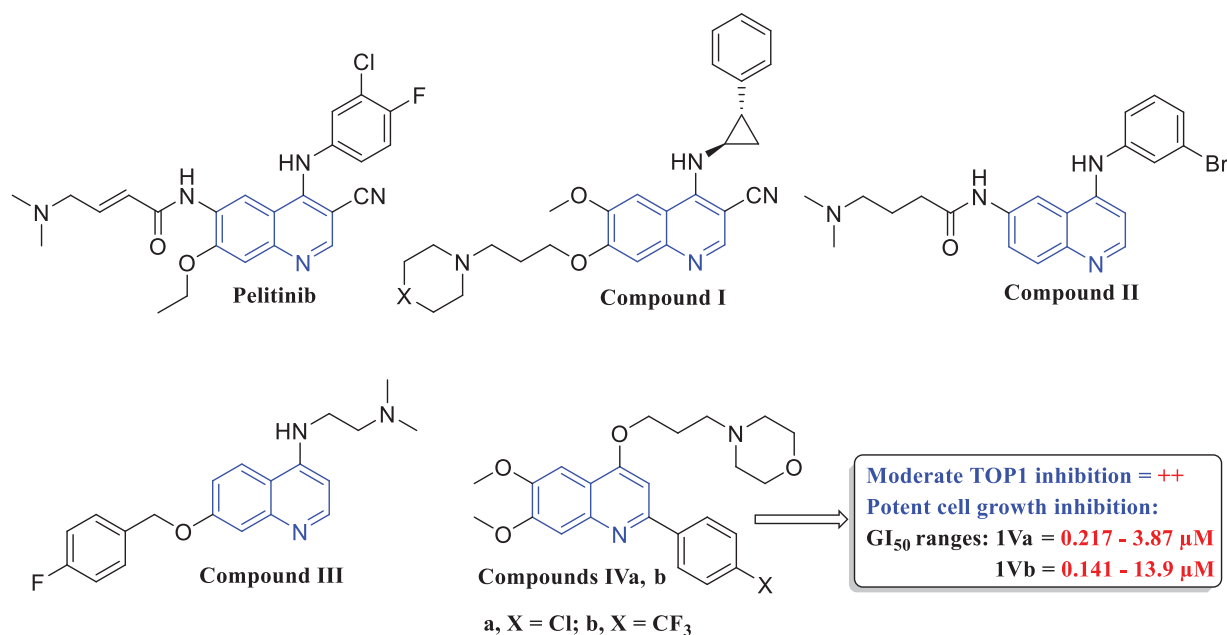


Figure 2. Some reported quinolines with potential anticancer activity.

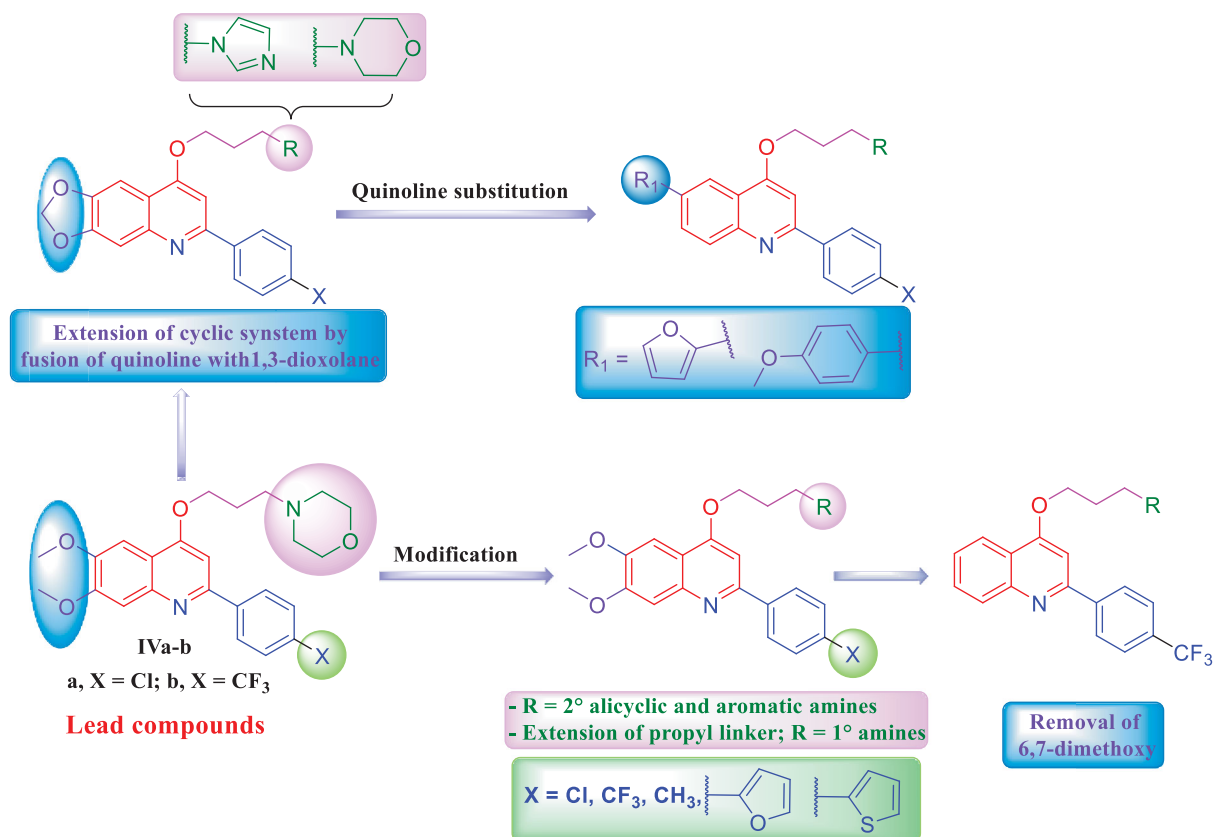


Figure 3. Different structural modification strategies adopted for design of target quinoline derivatives in this study.

arylquinolines (**6a–o**, **8a,b**, **10a,b**, **12a–d**, and **16a–d**) and 4-propoxy-2,6-diarylquinolines (**20a–f**) against various kinases (EGFR, FAK, FRK, IGF-1R, BTK, c-Src, VEGFR-1, VEGFR-2, HER-2). Strikingly, the investigated quinolines exhibited promising dual inhibitory effect towards EGFR and FAK kinases. Moreover, the apoptotic impact of the most potent anti-proliferative agents in this study was investigated on DLD-1 cells exploiting AV/PI dual staining assay. Finally, *in silico* molecular modelling techniques, including docking and molecular dynamics studies, were exploited to justify and support results obtained from the biological evaluations.

2. Results and discussion

2.1. Chemistry

The synthetic routes adopted for the synthesis of the target 4-propoxy-2-arylquinolines (**6a–o**, **8a,b**, **10a,b**, **12a–d**, **16a–d**) and 4-propoxy-2,6-diarylquinolines **20a–f** are illustrated in Schemes 1–3. Regarding Scheme 1, the benzamides **3a–c** were prepared by reacting 4,5-dimethoxy-2'-aminoacetophenone **1** with *p*-substituted benzoyl derivatives **2a–c** in dry THF and Et₃N. The latter were cyclized in refluxing dioxane and NaOH to afford the corresponding quinolones **4a–c** in excellent yields which then were subjected to *O*-alkylation with 1-bromo-3-chloropropane using our previously confirmed procedure to yield the respective 4-propoxy key intermediates **5a–c**³⁶. Finally, these key intermediates **5a–c** were converted to the target 4-propoxy-2-arylquinolines **6a–o** in good to excellent yields (70–80%) through nucleophilic substitution with the appropriate amine in dry DMF and potassium carbonate anhydrous using catalytic amount of potassium iodide at 90 °C.

In Scheme 2(A), the bromo analog of 4-propoxy-*N*-methylpiperazine-2-arylquinoline **7** was obtained based on the same pathway

for **6a–o** using *p*-bromobenzoyl chloride. Then, this bromo analog **7** has been transformed into the target heterocyclic derivatives **8a,b** in good yields (70–72%) under Suzuki cross coupling conditions through its reaction with the appropriate boronic acid derivative in dioxane using tetrakis catalyst and 2M sodium carbonate under N₂ at 90 °C. In Scheme 2(B,C), syntheses of the target demethoxylated analogs **10a,b** and 1,3-dioxolo analogs **12a–d** have been accomplished in good to excellent yields (72–87%) adopting the same synthetic routes described for **6a–o** using the respective starting compounds, intermediates, and amines.

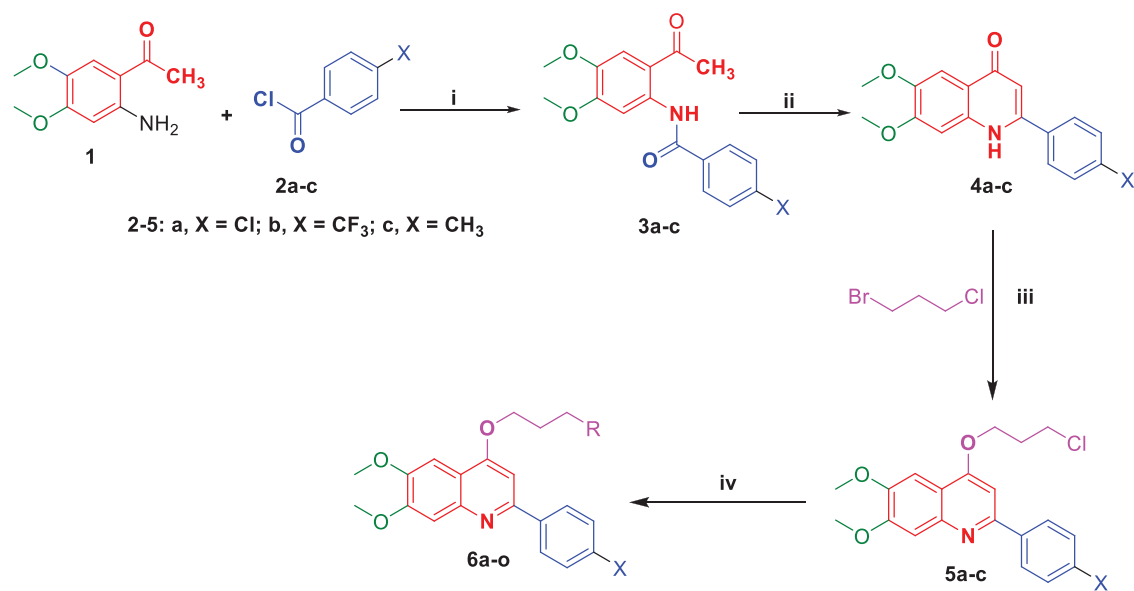
Concerning Scheme 3, initiated from 5-bromo-2'-aminoacetophenone **13**, the target 6-bromo analogs **16a–d** have been afforded in good to excellent yields (78–87%) applying the synthetic routes utilised for **6a–o**. Moreover, 5-bromo-2'-aminoacetophenone **13** was transferred to the 6-aryl derivatives **17a,b** via Suzuki coupling reaction by its reaction with the appropriate boronic acid derivative in dioxane/water in the presence of tetrakis catalyst and potassium carbonate under N₂ at 100 °C. Subsequently, these 6-aryl derivatives **17a,b** have been similarly converted to the target 4-propoxy-2,6-diarylquinolines **20a–f** in good to excellent yields (74–89%) exploiting the same experimental pathways adopted for **6a–o**.

The structures of all synthesised compounds have been authenticated employing one-dimensional (1D) and two-dimensional (2D) NMR (for 2D NMR, see Supplementary Data), in addition to high resolution mass spectrometry (HRMS).

2.2. 2.2. In vitro anticancer activity

2.2.1. Antiproliferative activity against different cancer cell lines

The *in vitro* antiproliferative activity of the synthesised 4-propoxy-2-arylquinolines (**6a–o**, **8a,b**, **10a,b**, **12a–d**, and **16a–d**) and 4-



6	X	R	6	X	R	6	X	R	6	X	R	6	X	R
a	Cl		b	Cl		c	Cl		d	Cl		e	Cl	
f	CF ₃		g	CF ₃		h	CF ₃		i	CF ₃		j	CF ₃	
k	CH ₃		l	CH ₃		m	CH ₃		n	CH ₃		o	CH ₃	

Scheme 1. Synthesis of target 4-propoxy-2-arylquinolines **6a–o**; Reagents and conditions: (i) Et₃N, THF, 0 °C then rt, overnight; (ii) dry dioxane, NaOH, reflux under N₂, 110 °C, 4 h; (iii) KI, KOH, 1-Bromo-3-chloropropane, dry DMF, rt, 24 h; (iv) KI, K₂CO₃ anhydrous, appropriate amine, dry DMF, reflux, 90 °C, 12 h.

propoxy-2,6-diarylquinolines (**20a–f**) was preliminary investigated by their screening at one dose level (10 μM) against five cancer cell lines representing three cancer types; colorectal cancer (DLD-1 and HCT-116), breast cancer (MDMBA-231 and MCF-7) and cervical cancer (HeLa). After the incubation of the tested compounds for 24 h, the percent growth inhibition (GI%) was calculated. For DLD-1 cell line, twelve compounds exerted good to excellent growth inhibition ranging from 71.94 to 95.36%, from them compounds **6f**, **6h**, **6i**, **16d**, **20e**, and **20f** displayed the highest GI%. Similarly, HCT-116 cell line established good to excellent sensitivity to the tested compounds and thirteen compounds exhibited GI% ranging from 64.26 to 97.48%, from them compounds **6d**, **6f**, **6h**, **6i**, **12c**, **16b**, **16d**, **20e**, and **20f** demonstrated the best sensitivity (Table 1).

Regarding breast cancer cell lines, GI% ranged from 75.34 to 84.76% and 71.97 to 87.36% for MDMBA-231 and MCF-7 cell lines, respectively. While five compounds showed good inhibitory activity towards MDMBA-231, ten compounds possessed good inhibition to the growth of MCF-7 cancer cell line. For HeLa cell line, seven compounds had good GI% from 65.73 to 90.78%. Based on the preceding screening results, it was revealed that colorectal cancer cell lines (DLD-1 and HCT-116) were the most sensitive to the tested compounds, therefore they were selected for further antiproliferative assay at six doses levels (Table 1).

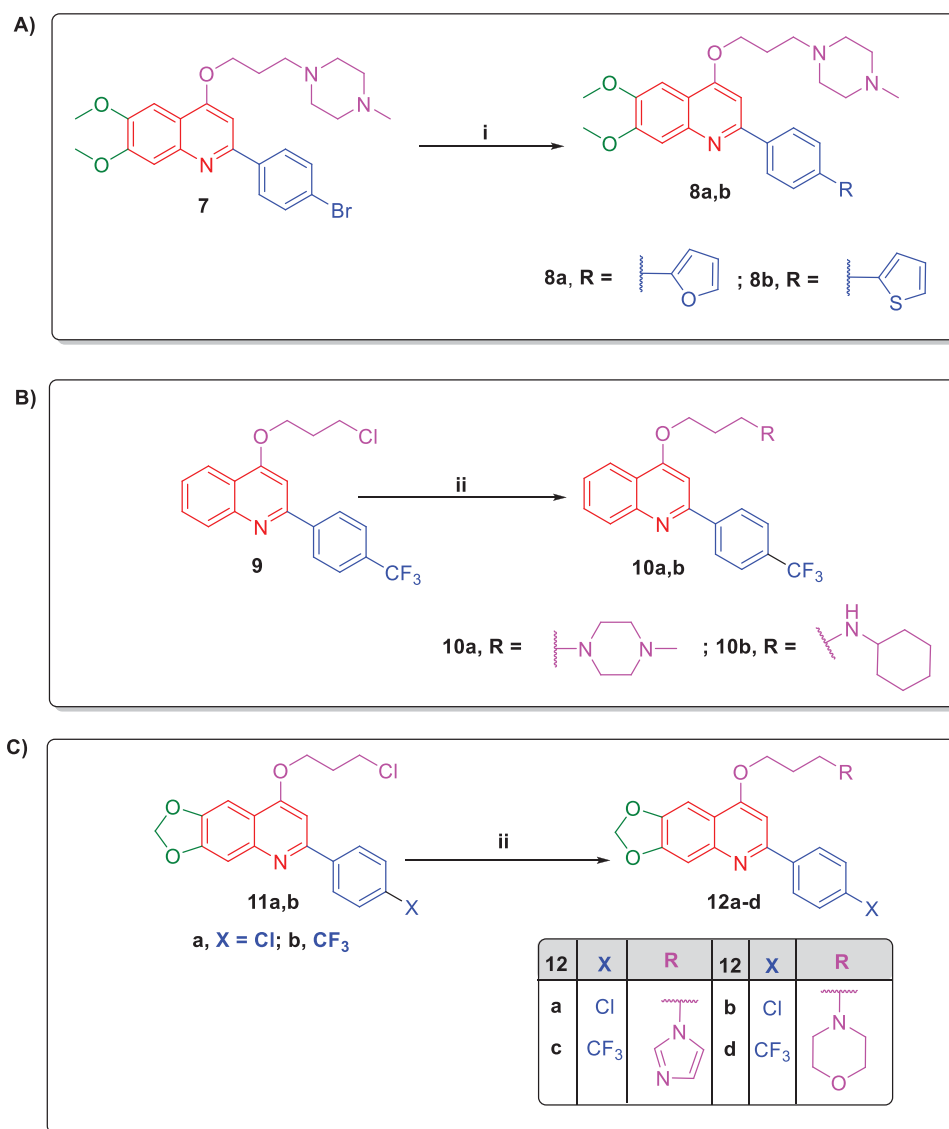
The growth inhibitory activity of the tested 4-propoxy-2-arylquinolines (**6a–o**, **8a,b**, **10a,b**, **12a–d**, and **16a–d**) and 4-propoxy-2,6-diarylquinolines **20a–f** exerted on the colorectal cancer cell lines (DLD-1 and HCT-116) was assessed using MTT assay. DLD-1 and HCT-116 cell lines were incubated for 24 h with increasing concentrations (0.5, 1, 10, 30, 50, and 100 μM) of the tested compounds. Gefitinib (EGFR inhibitor) and TAE226 (FAK inhibitor) were

used as reference drugs. The results were presented as half maximal growth inhibitory concentration (IC₅₀) which represents the concentration of a drug exhibiting 50% growth inhibition of the cell line compared to the negative control (Table 2).

The antiproliferative investigations against DLD-1 revealed that compound **6h** emerged as the most potent counterpart showing IC₅₀ = 1.79 μM surpassing the activity of Gefitinib by 5-folds which possessed IC₅₀ = 10.24 μM. Thereafter, compounds **6f**, **6i**, **16d**, and **20f** displayed 4-folds superior activity compared to Gefitinib with IC₅₀ values = 2.25, 2.48, 2.18, and 2.09 μM, respectively. In addition, compounds **6d**, **6l**, **6n**, **8b**, **12b**, **12c**, **16a**, **16b**, **20b**, and **20e** exerted better inhibitory activity than Gefitinib demonstrating IC₅₀ values = 8.15, 6.34, 6.11, 7.34, 8.36, 9.12, 8.22, 8.69, 9.65, and 4.46 μM, respectively. The rest of compounds had week to moderate or no activity relative to Gefitinib.

Concerning HCT-116 cell line, it was found that compounds **6f**, **6h**, **16d**, and **20f** established twice inhibitory activity compared to Gefitinib (IC₅₀ = 6.94 μM) displaying IC₅₀ values = 3.09, 3.28, 2.43, and 2.96 μM, respectively. Furthermore, compounds **6d**, **6i**, **12c**, **16a**, **16b**, and **20e** exhibited higher growth inhibitory activities than Gefitinib with IC₅₀ values = 4.67, 5.68, 6.37, 6.15, 4.22, and 4.75 μM, respectively. The remaining compounds possessed week to moderate or no activity compared to Gefitinib.

It is noteworthy that appending *p*-CF₃ to the 2-phenyl enhanced the antiproliferative activity compared to *p*-Cl and *p*-CH₃, except for the cyclohexylamine analogs **6b**, **6g**, and **6l** in which the *p*-CH₃ substituent is preferred for antiproliferative activity. Remarkably, the incorporation of *p*-(2-furyl) to the 2-phenyl abolished the growth inhibitory activity, while the introduction of *p*-(2-thienyl) increased the activity compared to *p*-Cl and *p*-CH₃ analogs. In the context of impact of amine substituents on the



Scheme 2. Synthesis of target 4-proxy-2-arylquinolines (A) **8a,b**; (B) **10a,b**; (C) **12a-d**; Reagents and conditions: (i) Pd(PPh₃)₄, 2 M Na₂CO₃, Arylboronic acid, dioxane, 90 °C under N₂, 16 h. (ii) KI, K₂CO₃ anhydrous, the respective amine, dry DMF, reflux, 90 °C, 12 h.

antiproliferative activity, it was proved that 4-amino-*N*-methylpiperidine is preferred for anticancer activity, then piperazine, tetrahydrofurfurylamine and cyclohexylamine. Notably, grafting imidazole along with 6,7-dimethoxy substituents abolished the antiproliferative activity for all derivatives.

Besides, the removal of 6,7-dimethoxy groups from the quinoline scaffold decreased or abolished activity. While the fusion of 1,3-dioxolo to the quinoline scaffold along with *p*-CF₃ substitution on phenyl dramatically potentiated the anticancer activity of the imidazole derivatives, the replacement of imidazole with morpholine decreased the activity of *p*-CF₃ analogs and markedly increased the activity of *p*-Cl counterparts. On the other hand, appending of electron withdrawing (Br) to position 6 of quinoline parallel with *p*-Cl substitution on 2-phenyl greatly enhanced the activity of the imidazole derivatives while, *p*-F substitution on the 2-phenyl extremely decreased the anticancer activity of imidazole derivatives. Also, the replacement of imidazole with morpholine almost had no impact on the *p*-Cl analogs, but tremendously elevated the anticancer activity of *p*-F derivatives.

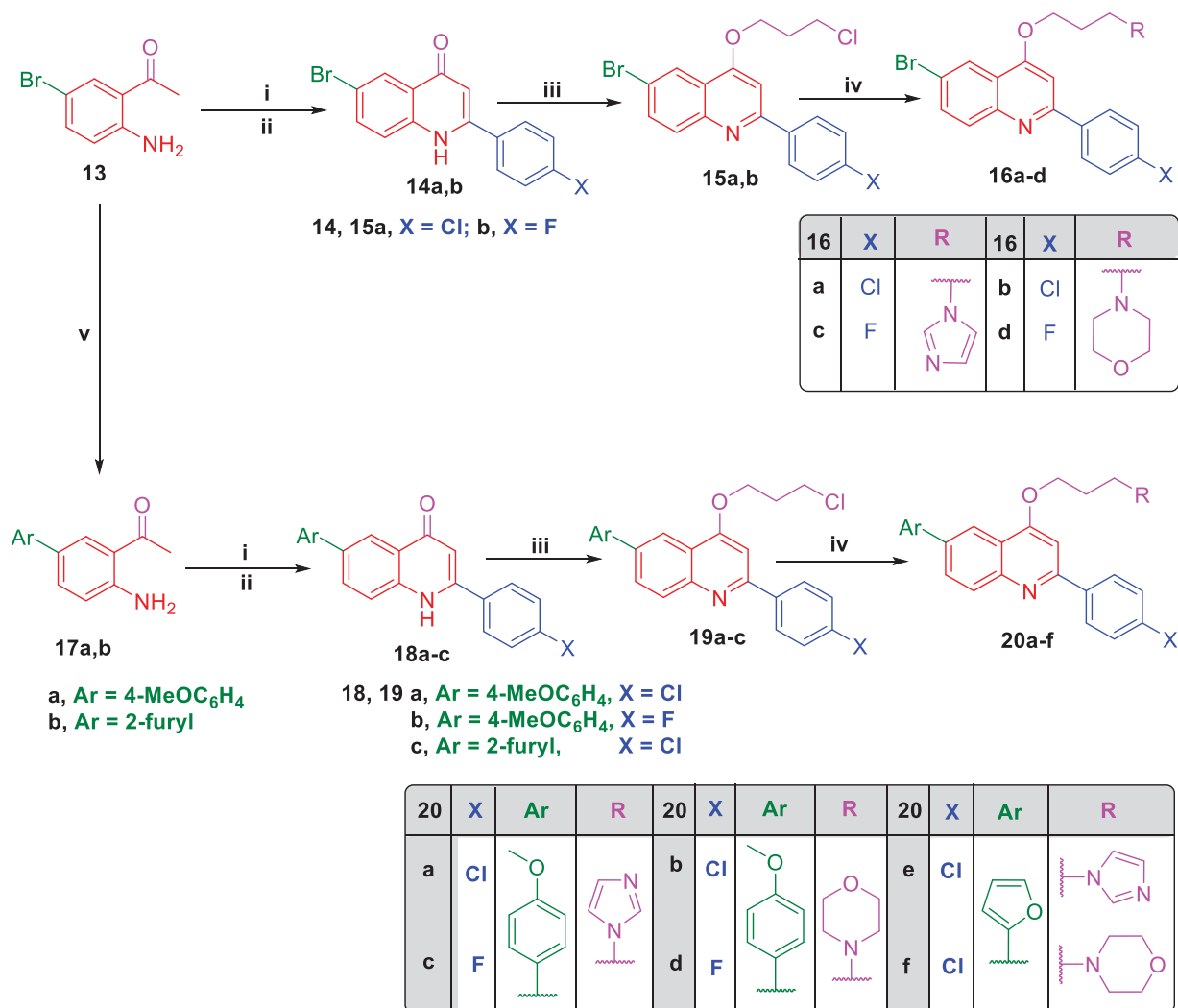
Furthermore, the incorporation of 4-methoxyphenyl or 2-furyl to position 6 of quinoline along with *p*-Cl or F on the 2-phenyl

enhanced the activity of the imidazole derivatives compared to the dimethoxy analogs, but the 2-furyl derivatives exhibited better activity. Moreover, the replacement of imidazole with morpholine elevated the antiproliferative activity of *p*-Cl analogs while, diminished the activity of *p*-F derivatives.

Finally, the deduced structure activity relationships indicated that the substitution pattern on positions 6 and 7 of quinoline and position 4 of the 2-phenyl, in addition to the amine substitution on the 4-proxy linker are crucial elements for the anticancer activity. In general, incorporation of dimethoxy groups at positions 6 and 7 of quinoline along with *p*-CF₃ at 2-phenyl and 4-amino-*N*-methylpiperidine, piperazine or tetrahydrofurfurylamine on the 4-proxy linker, in addition to grafting of electron withdrawing (Br) or 2-furyl at position 6 of quinoline along with *p*-F or Cl on the 2-phenyl and morpholine on the propoxy linker resulted in the most potent antiproliferative agents in this study.

2.2.2. Annexin V-FITC/propidium iodide apoptosis assay (AV/PI)

The apoptotic impact of the most potent antiproliferative agents **6f**, **6h**, **6i**, **16d**, and **20f** on DLD-1 colorectal cancer cell line was



Scheme 3. Synthesis of the target 6-bromo-4-propoxy-2-arylquinolines **16a–d** and 4-propoxy-2,6-diarylquinolines **20a–f**; Reagents and conditions: (i) the respective benzoyl chloride, Et₃N, THF, 0 °C then rt, overnight; (ii) dry dioxane, NaOH, reflux under N₂, 110 °C, 4 h; (iii) KI, KOH, 1-Bromo-3-chloropropane, dry DMF, rt, 24 h; (iv) KI, K₂CO₃ anhydrous, the respective amine, dry DMF, reflux, 90 °C, 12 h; (v) K₂CO₃, Pd(PPh₃)₄, Arylboronic acid, dioxane/H₂O (1:1), 100 °C under N₂, 4 h.

investigated exploiting AV/PI dual staining assay. The assay outcomes proved that the tested compounds elicited apoptosis of such cell line as indicated by significant rise in the total percentage of AV positive apoptotic DLD-1 cells compared to the control (Figure 4). Compound **6h** increased the total percentage of apoptotic cells from 7% for the control to 90.33%. Also, compounds **6f**, **6i**, **16d**, and **20f** exerted potential apoptotic effect elevating the total percentage of apoptotic cells to 84.33, 71.66, 51.66, and 80.66%, respectively.

2.3. Topoisomerase I-mediated DNA cleavage assay

TOP1 poisoning activity of all target compounds has been estimated utilising TOP1-mediated DNA cleavage assay that determines the TOP1 poisoning activity relative to 1 μM Camptothecin (CPT)³⁷. The tested compounds were incubated at 0.1, 1, 10, and 100 μM with recombinant human TOP1 enzyme and a 3'-[³²P]-labeled 117-bp DNA oligonucleotide³⁸. TOP1 poisoning agents specifically trap TOP1ccs leading to their stabilisation and DNA cleavage. The drug-induced stabilised TOP1ccs are visualised by gel electrophoresis demonstrating specific DNA cleavage patterns. Then a semiquantitative scoring system by visual comparison between lanes induced by the target compounds and 1 μM CPT

was used to score the compounds (Table 3, see Supplementary Data for the results of gel electrophoresis)^{39–41}.

Compounds **6a–e**, **6h**, **6i**, **6m**, **12a**, and **12b** exhibited weak TOP1 poisoning effect (-/+) displaying DNA cleavage activity equal to 0–25% of the activity of 1 μM CPT, while compound **16c** demonstrating activity (+) equals to 25–50% of the activity of 1 μM CPT. The rest of compounds possessed no cleavage activity. Despite the target compounds showing promising antiproliferative activity against cancer cell lines, their TOP1 poisoning activities were not encouraging for further development as potent TOP1 inhibitors. Accordingly, the synthesised compounds have been evaluated for the plausible mechanism by which they provoked the antiproliferative activity.

2.4. Kinase inhibitory activities of target quinolines

2.4.1. Kinase profiling

The non-significant TOP1 poisoning activities of target compounds obtained from Topoisomerase I-mediated DNA cleavage assay motivated us to search for the plausible molecular mechanism for herein reported 4-propoxy-2-arylquinolines.

The potential inhibitory activity of the target 4-propoxy-2-arylquinolines (**6a–o**, **8a,b**, **10a,b**, **12a–d**, **16a–d**) and 4-propoxy-2,6-

diarylquinolines (**20a–f**) was explored against a panel of nine kinases representing different signalling pathways; EGFR, FAK, FRK, IGF-1R, BTK, c-Src, VEGFR-1, VEGFR-2 and HER-2 (see [Supplementary Data, Table S1](#)). The half maximal inhibitory concentration (IC₅₀) values were calculated for each kinase and presented in [Table S1](#) and [Table 4](#). Strikingly, the screening outcomes revealed that the investigated quinolines exhibited promising dual inhibitory effect towards EGFR and FAK kinases.

Table 1. % Growth inhibition (GI%) of all target compounds **6a–o**, **8a,b**, **10a,b**, **12a–d**, **16a–d**, and **20a–f** against different cancer cell lines at 10 μM dose level.

Compounds	GI%				
	DLD1	HCT-116	MDMBA-231	MCF-7	Hela
6a	22.56	31.34	9.38	17.34	20.15
6b	36.25	42.81	19.67	23.49	12.81
6c	28.22	41.36	19.38	15.76	4.96
6d	75.64	82.61	63.39	71.97	26.98
6e	15.79	22.03	4.67	5.34	22.36
6f	95.36	88.46	75.34	94.36	69.17
6g	25.36	22.16	48.15	76.38	46.28
6h	92.36	89.34	84.76	90.36	90.78
6i	88.76	82.11	81.60	89.49	78.64
6j	6.31	2.46	8.42	14.67	5.67
6k	18.69	22.15	8.64	17.49	11.32
6l	75.34	69.15	38.36	44.71	34.29
6m	22.16	24.31	8.16	22.09	30.19
6n	81.34	64.26	14.39	58.15	71.12
6o	12.36	1.08	8.64	5.36	9.16
8a	5.15	1.02	4.40	7.22	11.78
8b	74.25	52.10	36.87	74.90	50.81
10a	22.51	18.64	37.15	14.26	25.64
10b	35.72	24.10	45.35	64.81	55.49
12a	21.25	16.25	4.98	11.72	22.79
12b	72.95	31.28	14.28	64.38	25.39
12c	71.94	80.49	61.94	43.27	68.22
12d	22.58	54.37	9.36	26.54	36.67
16a	60.08	76.17	51.24	22.97	47.35
16b	55.82	87.61	45.31	19.38	35.94
16c	12.25	18.14	20.11	4.36	8.67
16d	90.11	97.48	80.24	86.38	85.67
20a	44.98	36.71	29.08	15.23	22.06
20b	53.15	71.05	48.31	29.37	34.02
20c	41.34	38.64	32.11	76.82	22.08
20d	24.65	36.91	27.05	15.34	11.97
20e	90.65	89.64	56.29	73.61	65.73
20f	94.18	91.37	82.58	87.36	79.64

2.4.2. EGFR and FAK kinase inhibitory activity

All the newly prepared 4-propoxy-2-arylquinolines (**6a–o**, **8a,b**, **10a,b**, **12a–d**, and **16a–d**) and 4-propoxy-2,6-diarylquinolines (**20a–f**) were examined for their potential EGFR and FAK inhibitory activities. Gefitinib and TAE-226 were used as reference EGFR and FAK inhibitors, respectively. The results are reported as half maximal inhibitory concentration values (IC₅₀), as determined from triplicate measurements and are presented in [Table 4](#).

Results in [Table 4](#) revealed that the examined quinolines displayed moderate to potent inhibitory activity towards EGFR (IC₅₀ values ranging between 20.15 ± 1.07 and 485.46 ± 11.37 nM, [Table 4](#)). In particular, trifluoromethyl phenyl-bearing 6,7-dimethoxy-2-arylquinolines **6f**, **6h**, and **6i**, as well as 6-furanyl-2-arylquinoline **20f** emerged as the most efficient EGFR inhibitors with two-digits nanomolar IC₅₀s (IC₅₀ = 25.39 ± 3.49, 20.15 ± 1.07, 22.36 ± 2.05, and 24.81 ± 2.71 nM, respectively). Notably, these four derivatives displayed 2-fold higher activity than the reference EGFR inhibitor Gefitinib (IC₅₀ = 48.52 ± 3.64 nM). In addition, compounds **6b**, **6d**, **6l**, **6n**, **8b**, **16d**, and **20e** exhibited potent EGFR inhibitory activity, as the measured IC₅₀ values ranged between 33.65 ± 1.02 and 46.37 ± 4.09 nM, which are slightly improved or comparable to that of the reference drug Gefitinib ([Table 4](#)). Moreover, compounds **6c** and **12b** showed 2-fold decreased activity (IC₅₀ = 85.67 ± 6.46 and 95.36 ± 2.05 nM, respectively) than Gefitinib against EGFR. The remaining examined quinolines possessed moderate EGFR inhibitory activity (IC₅₀ range: 121.74 ± 9.40–485.46 ± 11.37 nM) compared to Gefitinib ([Table 4](#)). Strikingly, the inclusion of 4-amino-*N*-methylpiperidine, tetrahydrofurfurylamine and *N*-methylpiperazine along with 2-(*p*-CF₃ phenyl) and 6,7-dimethoxy substituents (**6f**, **6h**, and **6i**), in addition to the grafting of morpholine together with 2-(*p*-Cl phenyl) and 6-(2-furyl) **20f** afforded the most potent EGFR inhibitors in this study displaying IC₅₀ range from 20.15 ± 1.07 to 25.39 ± 3.49 nM.

On the other hand, as depicted in [Table 4](#), FAK kinase was efficiently inhibited by all 4-propoxy-2-arylquinolines (**6a–o**, **8a,b**, **10a,b**, **12a–d**, and **16a–d**) and 4-propoxy-2,6-diarylquinolines (**20a–f**) herein reported in the nanomolar range (IC₅₀ range: 14.25 ± 2.72–298.74 ± 1.94 nM). Superiorly, *p*-CF₃-phenyl-bearing 6,7-dimethoxy-2-arylquinolines **6f**, **6h**, and **6i**, as well as, morpholine-bearing 6-bromo-2-arylquinoline **16d** and 6-furanyl-2-arylquinoline **20f** were the most potent FAK inhibitors in this study with

Table 2. The half maximal growth inhibitory concentration (IC₅₀) of all target compounds **6a–o**, **8a,b**, **10a,b**, **12a–d**, **16a–d**, and **20a–f** against two colorectal cancer cell lines (DLD1 and HCT-116) compared to Gefitinib and TAE226.

Compounds	IC ₅₀ (μM) ^a		Compounds	IC ₅₀ (μM)	
	DLD1	HCT-116		DLD1	HCT-116
6a	>100	65.36 ± 4.37	10b	40.28 ± 2.09	>100
6b	19.37 ± 2.15	16.79 ± 1.56	12a	>100	>100
6c	46.95 ± 2.46	13.70 ± 1.29	12b	8.36 ± 1.08	14.36 ± 3.69
6d	8.15 ± 1.05	4.67 ± 0.85	12c	9.12 ± 2.11	6.37 ± 1.09
6e	>100	>100	12d	74.94 ± 5.46	9.20 ± 2.49
6f	2.25 ± 0.96	3.09 ± 1.05	16a	8.22 ± 1.12	6.15 ± 1.30
6g	75.36 ± 5.46	46.82 ± 3.16	16b	8.69 ± 2.64	4.22 ± 1.05
6h	1.79 ± 0.21	3.28 ± 0.67	16c	>100	88.05 ± 5.24
6i	2.48 ± 0.86	5.68 ± 1.42	16d	2.18 ± 0.52	2.43 ± 0.71
6j	>100	>100	20a	13.05 ± 3.69	24.11 ± 2.46
6k	>100	>100	20b	9.65 ± 2.15	7.34 ± 1.82
6l	6.34 ± 0.52	8.11 ± 1.04	20c	15.97 ± 1.10	12.49 ± 3.05
6m	54.21 ± 2.11	43.08 ± 1.05	20d	65.30 ± 5.36	29.47 ± 4.15
6n	6.11 ± 1.80	8.69 ± 0.94	20e	4.46 ± 0.65	4.75 ± 1.02
6o	>100	>100	20f	2.09 ± 0.14	2.96 ± 0.12
8a	>100	>100	Gefitinib	10.24 ± 2.10	6.94 ± 1.24
8b	7.34 ± 1.22	9.84 ± 0.68	TAE226	0.12 ± 0.05	0.17 ± 0.04
10a	>100	>100			

^aIC₅₀ values are the mean of three separate experiments ± SD.

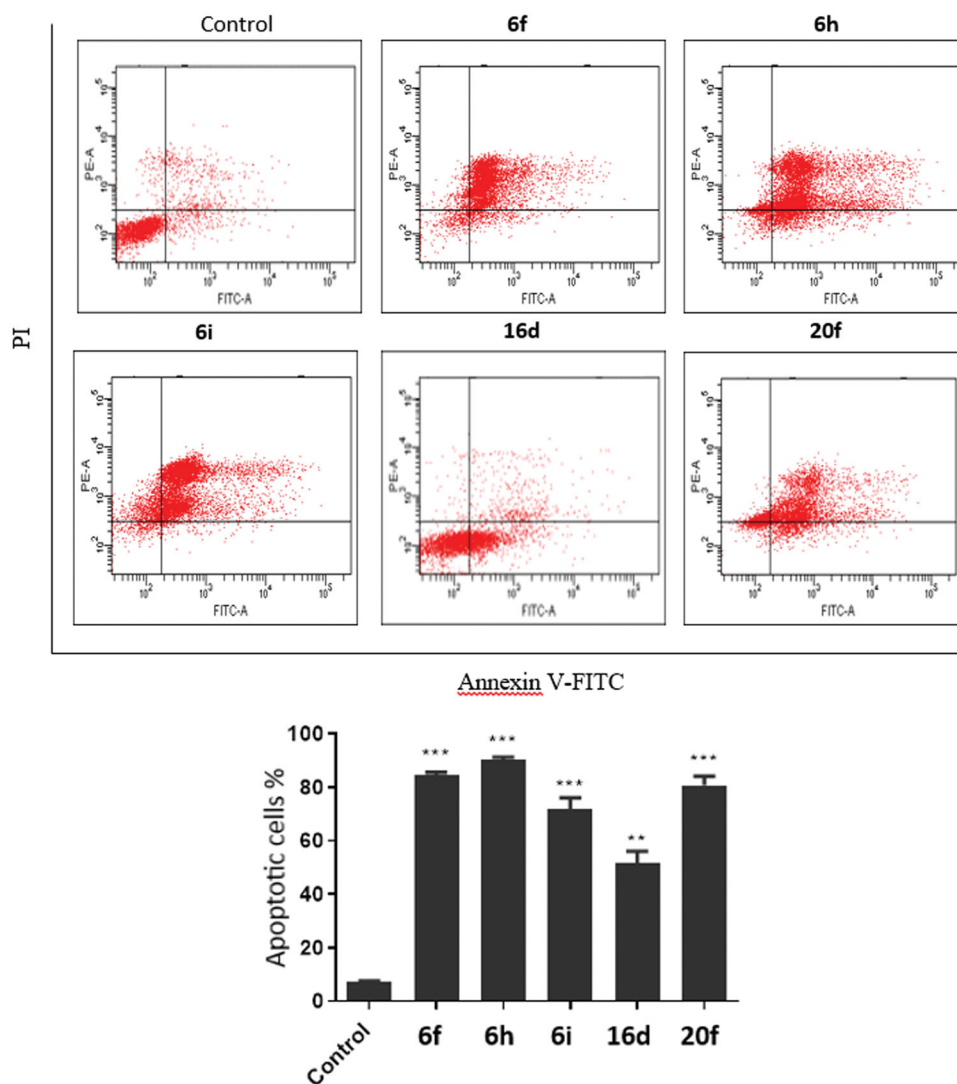


Figure 4. Influence of the promising compounds on the total percentage of AV-FITC positive staining in DLD1 cancer cell line.

IC_{50} values equal 22.68 ± 2.38 , 14.25 ± 2.72 , 18.36 ± 3.17 , 17.36 ± 2.15 , and 15.36 ± 0.98 nM, respectively (Table 4). Moreover, compounds **6c**, **6d**, **6i**, **6n**, **8b**, **16a**, **16b**, and **20e** exerted potent FAK inhibitory activity with IC_{50} spanning in the range 25.36 ± 3.48 – 50.36 ± 4.81 nM.

Further analysis of the obtained results in Table 4 revealed that compounds **6b**, **12b**, and **20a–c** exhibited two-digit nanomolar IC_{50} s; 98.16 ± 4.67 , 70.85 ± 3.16 , 77.25 ± 4.37 , 63.25 ± 3.25 , and 91.03 ± 5.85 nM, respectively, whereas the remaining derivatives displayed moderate inhibitory activity against FAK kinase (IC_{50} range: 111.06 ± 8.94 – 298.74 ± 1.94 nM) (Table 4). Interestingly, the incorporation of 4-amino-*N*-methylpiperidine, tetrahydrofurfurylamine and *N*-methylpiperazine along with 2-(*p*-CF₃ phenyl) and 6,7-dimethoxy substituents (**6f**, **6h**, and **6i**), besides the appending of morpholine with 2-(*p*-F phenyl) and 6-Br **16d**, as well as the addition of morpholine in conjunction with 2-(*p*-Cl phenyl) and 6-(2-furyl) **20f** provided the most potent FAK inhibitors in this study demonstrating IC_{50} values ranging from 14.25 ± 2.72 to 22.68 ± 2.38 nM.

It is worth stressing that 4-propoxy-2-arylquinolines **6f**, **6h**, **6i**, and **20f** emerged not only as the most potent dual EGFR/FAK inhibitors in this study, but also as the most efficient anti-proliferative agents towards the examined colorectal cancer (DLD-1 and HCT-116) cell lines.

2.5. In silico molecular docking

2.5.1. Docking into EGFR binding site

The molecular docking approach was utilised to investigate the potential binding of herein reported 4-propoxy-2-arylquinolines to EGFR binding site (PDB: 1M17). The docking procedure was validated through the redocking of the co-crystallised ligand. The correct pose was predicted accurately with RMSD of 1.498 between the docked and co-crystallised ligand using DockRMSD server (Figure 5(a))⁴². In addition, docking was able to maintain hydrogen bonding seen in the co-crystallised ligand with NH of M769 (2.7 Å) and with the NH of G772 (3.2 Å). Furthermore, hydrophobic interactions with residues in the active site were also maintained. These include interactions between K721 and ethyne benzene moiety, and L694, L768, and L820 with hydrophobic part of the quinazoline ring (Figure 5(b)).

Docking scores of the tested compounds with EGFR are shown in Table 5. The docking score of the co-crystallised ligand was -7.2 kcal/mol, whereas all the tested quinolines have shown better docking scores than that of the co-crystallised ligand (-7.9 to -9.7 kcal/mol). Best docking scores were seen with quinolines from the series **20**. Compound **20c** showed the best binding energy to EGFR with docking score of -9.7 kcal/mol and its binding pose is shown in Figure 5(c). The compound

has formed 2 hydrogen bonds between imidazole ring and both K721 (3.5 Å) and T766 (3.1 Å). Also, several hydrophobic interactions have been seen, which included interactions between quinoline ring and side chains of V702 and T830. The phenyl ring at position 2 formed hydrophobic interactions with L694 and L820 which are also common with the co-crystallised ligand. In addition, π - π stacking between the ring at quinoline position 6 and F699.

Another compound from this series is compound **20e** which was selected as a representative example because it has shown good biological results with both EGFR and FAK. The docking pose of this compound is shown in Figure 5(d) showing a similar docking pose to **20c**. The same hydrogen bonds with K721 (3.5 Å) and T766 (3.1 Å) were maintained as well as hydrophobic interactions with V702 and T830 as well as with L694 and L820. The π - π stacking was also seen between F699 and the furan ring of **20e**. This compound, in complex with EGFR, was subjected to further investigation using molecular dynamics to study the stability of its complex with EGFR as will be discussed later.

Table 3. The TOP1 inhibitory activity of all target compounds **6a–o**, **8a,b**, **10a,b**, **12a–d**, **16a–d**, and **20a–f** compared to Camptothecin (CPT).

Compounds	TOP1 inhibitory activity ^a	Compounds	TOP1 inhibitory activity
6a	–/+	10a	0
6b	–/+	10b	0
6c	–/+	12a	–/+
6d	–/+	12b	–/+
6e	–/+	12c	0
6f	0	12d	0
6g	0	16a	0
6h	–/+	16b	0
6i	0	16c	+
6j	0	16d	0
6k	0	20a	0
6l	–/+	20b	0
6m	–/+	20c	0
6n	0	20d	0
6o	0	20e	0
8a	0	20f	0
8b	0		

^aScoring: 0: no activity; –/+ : 0–25% 1 μ M CPT; +: 25–50% 1 μ M CPT.

2.5.2. Docking into FAK binding site

Potential binding of target quinolines to FAK was also investigated using docking studies (PDB: 2JKM). Initially, the docking procedure was validated through the redocking of the co-crystallised ligand (AZW592). The docking searching algorithm was able to correctly predict the binding pose with acceptable accuracy with RMSD of 1.318 between the docked and co-crystallised ligands as predicted by DockRMSD server (Figure 6(a))⁴². The docked structure was able to maintain same hydrogen bonds that are in the crystal structure including those between the sulphamoyl moiety oxygen and the terminal amino group of K454 (Å) and the hydrogen bond with the α -carbonyl group of C502. In addition, several hydrophobic interactions have been also seen with residues in the active site including I428, V436, V484, L501, and L553 (Figure 6(b)).

Next, target synthesised quinolines were docked in the active site of the FAK after their preparation. The docking scores of tested compounds are shown in Table 5. The docking score of co-crystallised ligand (AZW592) was found to be –8.5 kcal/mol. Some of tested compounds have shown scores that are comparable to the co-crystallised ligand. Best results were seen with **12** and **20** and some of the **16** series. Docking poses of these compounds were similar with most of the docked compounds as can be seen in Figure 6(c) which shows docking pose of some compounds from these series.

Docking pose of compound **20e** which was chosen as representative example is shown in Figure 6(d). The compound was able to form 3 hydrogen bonds with N551 (3.1 Å), D564 (3.1 Å), and E506 (3.3 Å). In addition, several hydrophobic interactions were also seen, such as the hydrophobic interaction between quinoline ring and L553 and between phenyl ring at position 2 and I428 which are common with the co-crystallized ligand. This pose was selected for further investigation of the complex stability using molecular dynamics study.

2.6. Molecular dynamics (MD) simulation

The stability of compound **20e** complexes with both EGFR and FAK was investigated using 100 ns molecular dynamics studies. With each complex, the results were compared with the

Table 4. The half maximal inhibitory concentration (IC₅₀) of all target compounds **6a–o**, **8a,b**, **10a,b**, **12a–d**, **16a–d**, and **20a–f** against EGFR and FAK kinase activity compared to Gefitinib and TAE226.

Compounds	IC ₅₀ (nM) ^a		Compounds	IC ₅₀ (nM)	
	EGFR	FAK		EGFR	FAK
6a	142.64 ± 2.54	214.36 ± 1.09	10b	179.64 ± 9.12	164.74 ± 5.37
6b	45.26 ± 5.36	98.16 ± 4.67	12a	124.97 ± 7.94	225.46 ± 14.02
6c	85.67 ± 6.46	45.70 ± 3.40	12b	95.36 ± 2.05	70.85 ± 3.16
6d	46.37 ± 4.09	36.97 ± 2.34	12c	246.70 ± 12.29	111.06 ± 8.94
6e	156.72 ± 11.36	211.08 ± 8.96	12d	450.16 ± 4.25	273.16 ± 2.84
6f	25.39 ± 3.49	22.68 ± 2.38	16a	222.15 ± 8.25	44.15 ± 3.26
6g	365.49 ± 14.82	145.71 ± 10.54	16b	313.34 ± 15.34	50.36 ± 4.81
6h	20.15 ± 1.07	14.25 ± 2.72	16c	485.46 ± 11.37	224 ± 10.46
6i	22.36 ± 2.05	18.36 ± 3.17	16d	35.03 ± 2.64	17.36 ± 2.15
6j	258.34 ± 11.94	186.46 ± 6.22	20a	121.74 ± 9.40	77.25 ± 4.37
6k	410.38 ± 12.73	157.84 ± 8.73	20b	245.11 ± 12.34	63.25 ± 3.25
6l	34.91 ± 3.76	26.37 ± 2.81	20c	362.30 ± 5.26	91.03 ± 5.85
6m	154.29 ± 12.80	172.49 ± 13.67	20d	146.95 ± 8.37	125.38 ± 3.15
6n	41.82 ± 2.34	44.36 ± 2.94	20e	33.65 ± 1.02	25.36 ± 3.48
6o	256.19 ± 6.94	204.84 ± 8.04	20f	24.81 ± 2.71	15.36 ± 0.98
8a	349.37 ± 14.05	198.32 ± 12.32	Gefitinib	48.52 ± 3.64	–
8b	35.48 ± 1.50	29.79 ± 2.37	TAE226	–	4.60 ± 0.94
10a	244.30 ± 8.41	298.74 ± 1.94			

^aIC₅₀ values are the mean of three separate experiments ± SD.

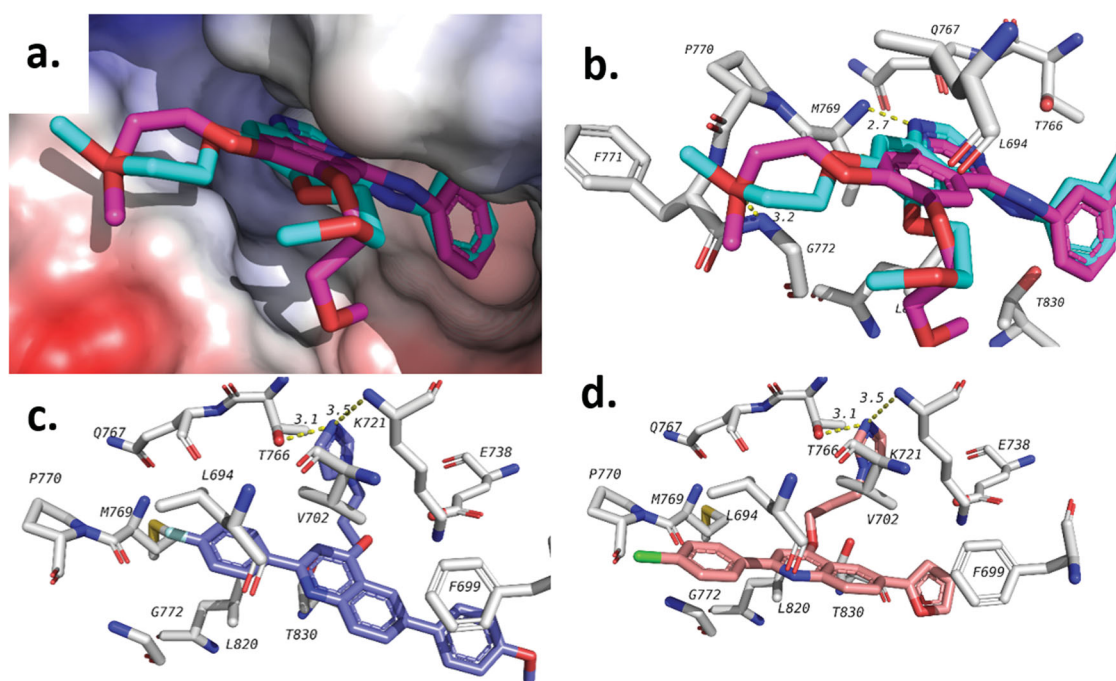


Figure 5. Docking of target quinolines in the active site EGFR. (a) validation of docking procedure showing overlapping of crystallised (blue) and docked (pink) poses; (b) interactions of Erlotinib with EGFR; (c) docking pose of **20c**; (d) docking pose of **20e**.

Table 5. Docking results of target compounds with EGFR and FAK.

Compound	Docking Score (kcal/mol)	
	EGFR (PDB: 1M17)	FAK (PDB: 2JKM)
6a	-8.1	-7.7
6b	-8.5	-7.3
6c	-8.2	-7.5
6d	-7.9	-7
6e	-8.4	-7.6
6f	-8.2	-7.4
6g	-8.5	-7.6
6h	-8.2	-7.6
6i	-8.1	-7.3
6j	-8.6	-8.0
6k	-8.1	-7.7
6l	-8.7	-7.4
6m	-8.3	-7.5
6n	-8.2	-7.1
6o	-8.4	-7.7
8a	-8.3	-7.6
8b	-8.4	-7.5
10a	-8.8	-7.9
10b	-8.3	-8.0
12a	-8.5	-8.0
12b	-8.5	-8.3
12c	-8.8	-8.4
12d	-8.7	-8.3
16a	-8.1	-7.7
16b	-8.2	-8.0
16c	-8.3	-7.7
16d	-8.3	-7.9
20a	-9.3	-8.3
20b	-9.1	-8.2
20c	-9.7	-8.3
20d	-9.2	-8.2
20e	-9.3	-8.2
20f	-8.8	-7.7
Co-crystallised ligand	-7.2 (Erlotinib)	-8.5 (AZW592)

co-crystallised ligand complex as a control and with the apo-protein (the protein alone with no ligands). The missing loops in both targets were built using Swiss-Model server⁴³ before starting the dynamics to ensure correct results. All complexes were

equilibrated under NVT then NPT conditions for 1 ns each and the analysis was done on the production run.

Analysis of the production runs trajectories for **20e** in the active site of EGFR demonstrated stability comparable to the co-crystallised ligand. Radius of gyration (R_g) is a measure of the compactness of the complexes. Stable R_g suggested the stability of the protein or complex under investigation. Figure 7(a) shows a plot of R_g of **20e**, co-crystallised ligand and apo-protein. The average R_g was found to be 2.01 ± 0.02 , 2.03 ± 0.02 , and 2.02 ± 0.01 nm for apo-protein, control, and **20e**, respectively. In addition, Root mean square fluctuation (RMSF) of protein residue (Figure 7(b)) for all the three complexes showing similar patterns. The average RMSF for co-crystallised ligand and **20e** was found to be 0.19 and 0.18 nm, respectively which is slightly higher than that of the apo-protein (0.15 nm). Although root mean square deviation (RMSD) of ligand heavy atoms for **20e** is slightly higher than that of the co-crystallised ligand (Figure 7(c)), the value is <1 nm for most of the trajectory. This value cannot be calculated for the apo-protein as it has no ligand in the system. Finally, the number of hydrogen bonds between ligands and protein are shown in Figure 7(d), which showed that **20e** formed extra hydrogen bonds during at least 50% of the production run time. These results suggested that **20e** complex with EGFR is at least of comparable stability when compared to the complex with the co-crystallised ligand; Erlotinib.

Complexes of FAK with **20e**, its co-crystallised ligand and the apo-protein showed similar pattern to that of the EGFR (Figure 8). This includes the radius of gyration (R_g), which showed an average of 2.00 ± 0.01 , 1.99 ± 0.01 , and 1.96 ± 0.01 nm for apo-protein, co-crystallised ligand, and **20e**, respectively (Figure 8(a)). Also, RMSF of protein residues was found to follow similar patterns for all the three studied systems (Figure 8(b)). The average RMSF for the three systems was found to be 0.12 ± 0.07 , 0.13 ± 0.09 , and 0.12 ± 0.07 nm for apo-protein, co-crystallised ligand, and **20e**, respectively. In addition, plotting of RMSD of ligand heavy atoms (Figure 8(c)) showed minimal fluctuation for both with and average RMSD of 0.19 ± 0.05 and

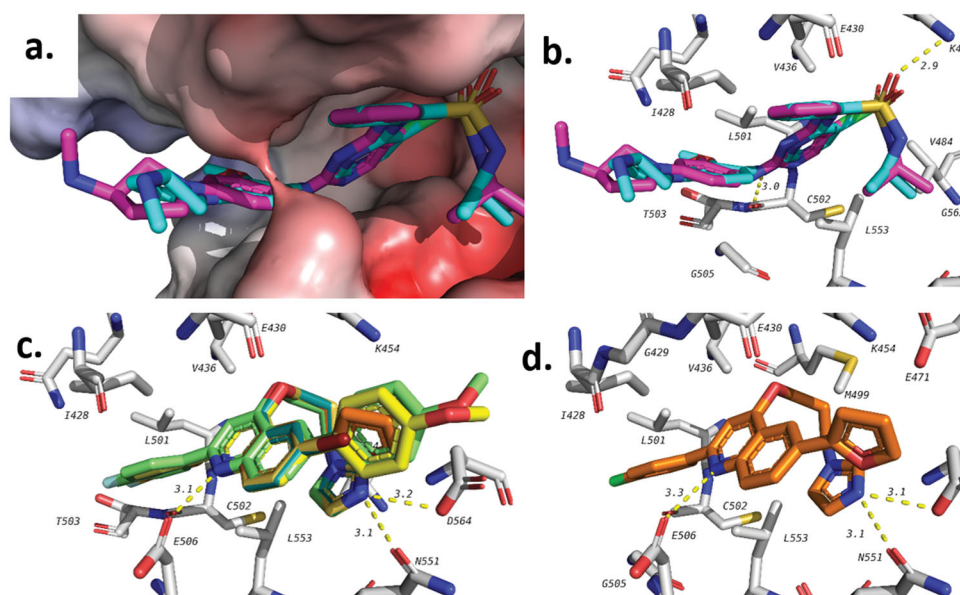


Figure 6. Docking of target compounds in the active site FAK. (a) validation of docking procedure showing overlapping of crystallised (blue) and docked (pink) poses; (b) interactions of AZW592 with FAK; (c) general binding of 16 and 20 compound series; (d) docking pose of 20e.

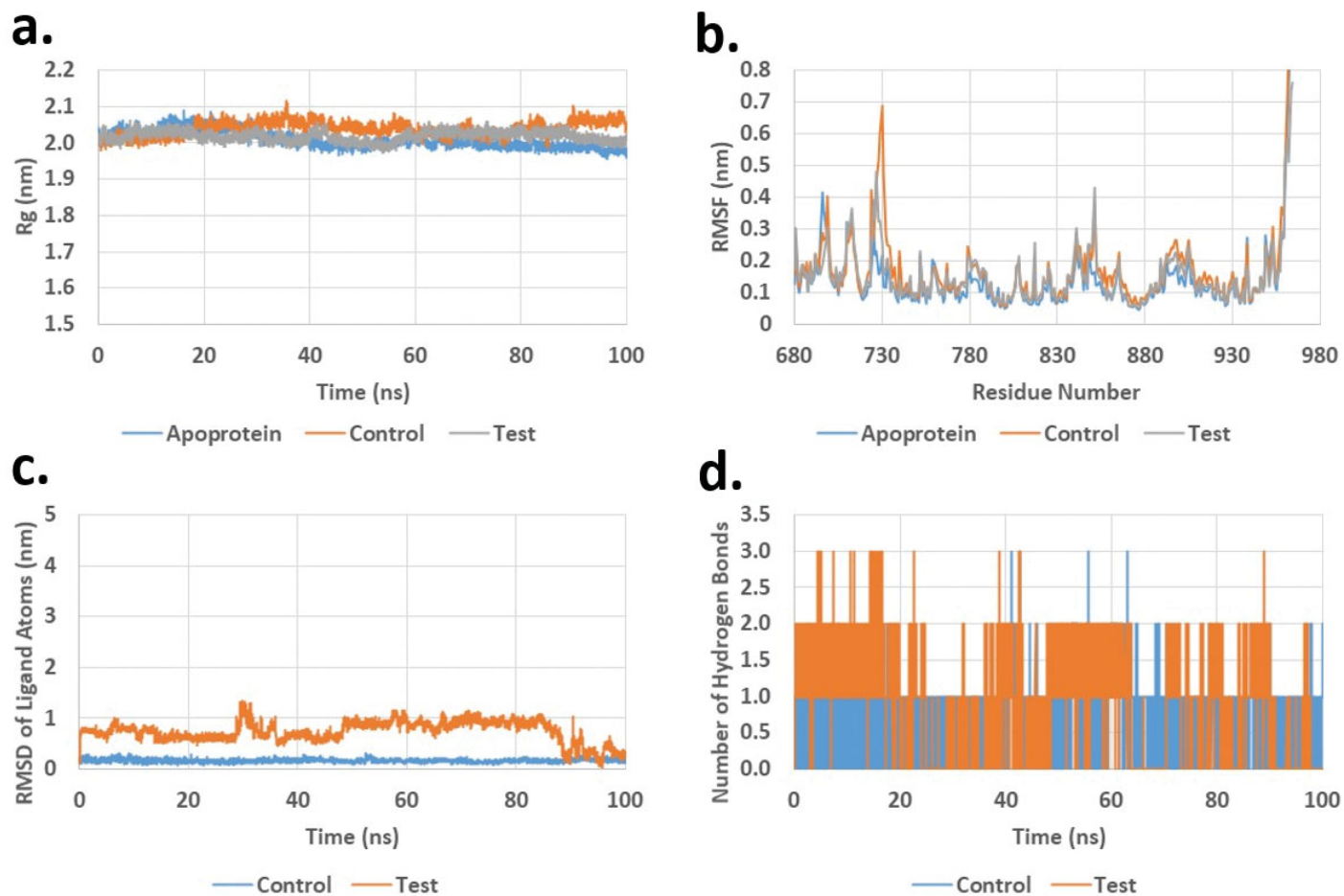


Figure 7. Molecular dynamics analysis of the production run trajectory of 20e in the active site of EGFR compared to control and apoprotein. (a) Radius of gyration; (b) Root mean square fluctuation of residues; (c) Root mean square deviation of ligand heavy atoms; (d) Number of hydrogen bonds between ligand and protein.

0.57 ± 0.16 nm for co-crystallised ligand and 20e, respectively. Although, the value for 20e is higher but it is within acceptable range (<1 nm). Finally, plotting of hydrogen bonds between ligands and target protein (Figure 8(d)) showed that the

number of hydrogen bonds is higher in case of the co-crystallised ligand compared to 20e. Being said, 20e was still able to maintain an average of 1.93 ± 0.45 hydrogen bonds during the 100 ns production run.

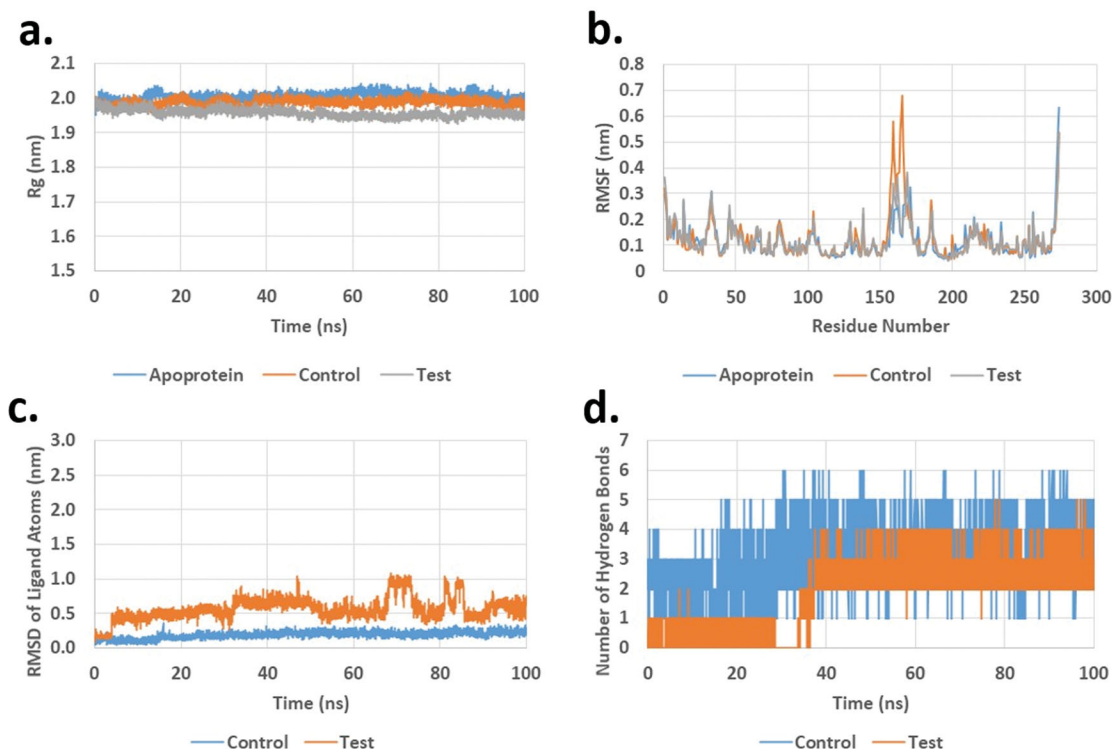


Figure 8. Molecular dynamics analysis of the production run trajectory of **20e** in the active site of FAK compared to control and apoprotein. (a) Radius of gyration; (b) Root mean square fluctuation of residues; (c) Root mean square deviation of ligand heavy atoms; (d) Number of hydrogen bonds between ligand and protein.

These results collectively suggested the stability of compound **20e** complexes with both EGFR and FAK compared to the corresponding co-crystallised ligands in each target. This in general supported the dual mechanism similar to the enzymatic inhibition data.

3. Conclusion

Different series of 4-propoxy-2-arylquinolines (**6a–o**, **8a,b**, **10a,b**, **12a–d**, and **16a–d**) and 4-propoxy-2,6-diarylquinolines (**20a–f**) have been designed and synthesised as potential anticancer agents. The quinolines **6f**, **6h**, **6i**, **16d**, and **20f** demonstrated the most potent antiproliferative effect against DLD-1 colorectal cancer with respective IC_{50} values = 2.25, 1.79, 2.48, 2.18, and 2.09 μ M with 4- to 5-folds potency compared to Gefitinib (IC_{50} = 10.24 μ M). Additionally, compounds **6f**, **6h**, **16d**, and **20f** possessed twice growth inhibitory impact as Gefitinib (IC_{50} = 6.94 μ M) displaying IC_{50} values = 3.09, 3.28, 2.43, and 2.96 μ M against HCT-116 cell line, respectively. Moreover, compounds **6f**, **6h**, **6i**, **16d**, and **20f** significantly elevated the total percentage of DLD-1 apoptotic cells. Furthermore, the quinolines **6f**, **6h**, **6i**, and **20f** exerted potent EGFR inhibitory effects with IC_{50} values = 25.39 ± 3.49 , 20.15 ± 1.07 , 22.36 ± 2.05 , and 24.81 ± 2.71 nM, respectively compared to Gefitinib (IC_{50} = 48.52 ± 3.64 nM). In a similar fashion, the quinolines **6f**, **6h**, **6i**, **16d**, and **20f** displayed the best FAK inhibitory actions with IC_{50} values = 22.68 ± 2.38 , 14.25 ± 2.72 , 18.36 ± 3.17 , 17.36 ± 2.15 , and 15.36 ± 0.98 nM, respectively. Molecular docking and molecular dynamics simulation rationalised EGFR/FAK dual inhibition providing different quinolines being as the first reported quinolines possessing potential EGFR/FAK dual inhibition. The latter compounds can be used as

lead compounds for the development of more potent EGFR/FAK dual inhibitors as potential anticancer agents.

4. Experimental

4.1. Chemistry

4.1.1. General

Melting points have been measured by Yanaco melting point device and were uncorrected. NMR spectra were measured using Bruker Advance III HD at 400 MHz for ^1H NMR, 100 MHz for ^{13}C NMR and 376 MHz for ^{19}F NMR in deuterated CDCl_3 or $\text{DMSO}-d_6$ using tetramethyl silane (TMS) as an internal standard. Coupling constant values (J) were determined in Hertz (Hz) and chemical shifts (δ) were expressed in ppm. High resolution mass spectrometry (HRMS) have been measured by Thermo Fisher Scientific LTQ Orbitrap XL spectrophotometer using electrospray ionisation (ESI) and the results were expressed as $[M+H]^+$ or $[M+Na]^+$ at Natural Science Research and Development Centre, Hiroshima University, Japan. The purities of all biologically tested compounds were determined by HPLC and were found to be $\geq 95\%$. HPLC analysis was performed utilising JASCO 880-PU HPLC system (Japan spectroscopic Co. Ltd) connected to a diode array detector with detection at a wavelength of 254 nm. The column exploited in the HPLC analysis was Inertsil ODS-3 column with dimensions of 250×4.6 mm and $5 \mu\text{m}$ particle size (GL SCIENCES INC., Japan). The mobile phase employed for HPLC analysis was acetonitrile/water/TFA (29.9/70/0.1, v/v) at a flow rate of 0.5 ml/min. The reactions have been monitored by thin layer chromatography (TLC) using Merck silica gel 60F₂₅₄ aluminium sheets. Column chromatography has been performed utilising silica gel 60N, 63–210 μm that was purchased from Kanto Chemical Co. Inc., Japan using

dichloromethane/methanol (100/0 to 90/10, v/v) and hexane/ethylacetate (100/0 to 90/10, v/v). Unless otherwise stated, all chemicals and solvents were available commercially and have been used without further purification.

4.1.2. Synthesis of 1-(2-amino-4,5-dimethoxyphenyl)ethan-1-one (1)

2'-Aminoacetophenone derivative **1** was prepared using the reported method^{44,45}.

Yellow solid, yield 70%, m.p. 100–102 °C; ¹H NMR (400 MHz, CDCl₃) δ (ppm): 2.53 (s, 3H, CH₃), 3.85 (s, 3H, OCH₃), 3.89 (s, 3H, OCH₃), 6.12 (s, 1H, phenyl CH), 6.27 (br s, 2H, NH₂), 7.12 (s, 1H, phenyl CH).

4.1.3. General procedure for the synthesis of benzamides (3a–c)

In dry THF (8 ml) and Et₃N (2 ml), 1-(2-amino-4,5-dimethoxyphenyl)ethan-1-one **1** (0.976 g, 5 mmol) was dissolved and cooled in ice bath. Then, a solution of the respective *p*-substituted benzoyl chloride **2a–c** (5.1 mmol) in dry THF (2 ml) was added dropwise while cooling in ice bath. The reaction mixture was stirred in ice bath for 30 min and then overnight at room temperature. After that, reaction mixture was poured into ice/water and the resulting solid was filtered off and washed excessively with water and methanol to afford the corresponding **3a–c**.

The spectral characterisation of the benzamides **3a,b** were reported in our previous study³⁶.

4.1.3.1. N-(2-acetyl-4,5-dimethoxyphenyl)-4-methylbenzamide (3c)

White solid, yield 70%, m.p. 165–167 °C; ¹H NMR (400 MHz, CDCl₃) δ (ppm): 2.42 (s, 3H, CH₃), 2.65 (s, 3H, CH₃C=O), 3.91 (s, 3H, OCH₃), 4.02 (s, 3H, OCH₃), 7.29 (d, 2H, benzoyl 2CH, *J* = 8.1 Hz), 7.30 (s, 1H, phenyl CH), 7.96 (d, 2H, benzoyl 2CH, *J* = 8.1 Hz), 8.77 (s, 1H, phenyl CH), 12.93 (s, 1H, NH); ¹³C NMR (100 MHz, CDCl₃) δ (ppm): 21.48, 28.37, 56.23, 56.43, 103.52, 113.90, 114.52, 127.45, 129.48, 132.01, 138.49, 142.49, 143.57, 154.89, 166.19 (C=O), 201 (C=O); HRESIMS (*m/z*): [M + H]⁺ Calcd for C₁₈H₂₀NO₄, 314.13868; found, 314.13901.

4.1.4. General procedures for synthesis of the quinolones (4a–c)

Under N₂ atmosphere, the benzamides **3a–c** and three equivalents NaOH were refluxed in dry dioxane at 110 °C for 4 h and then cooled to room temperature. Small amount of water and excess amount of hexane were added to the reaction mixture. The resulting mixture was subjected to sonication for 2 min and then neutralised using 1 M HCl. The separated solid was filtered off and washed excessively with water to give the corresponding quinolones **4a–c**.

The spectral data of the quinolones **4a,b** have been reported in our previous study³⁶.

4.1.4.1. 6,7-dimethoxy-2-(*p*-tolyl)quinolin-4(1H)-one (4c). Yellow solid, Yield 92%, m.p. > 250 °C; ¹H NMR (400 MHz, DMSO-*d*₆) δ (ppm): 2.43 (s, 3H, CH₃), 3.93 (s, 3H, OCH₃), 3.96 (s, 3H, OCH₃), 7.03 (s, 1H, vinyl CH), 7.47 (d, 2H, *p*-toluoyl 2CH, *J* = 8.1 Hz), 7.51 (s, 1H, phenyl CH), 7.62 (s, 1H, phenyl CH), 7.84 (d, 2H, *p*-toluoyl 2CH, *J* = 8.1 Hz); ¹³C NMR (100 MHz, DMSO-*d*₆) δ (ppm): 21.43, 56.39, 56.62, 100.57, 102.37, 104.13, 115.90, 128.22, 130.19, 130.34, 137.47, 142.04, 149.30, 151.20, 155.22, 170.10 (C=O); HRESIMS (*m/z*): [M + H]⁺ Calcd for C₁₈H₁₈NO₃, 296.12812; found, 296.12827.

4.1.5. General procedure for synthesis of the key intermediates (5a–c)

The quinolones **4a–c** (3 mmol), KI (0.498 g, 3 mmol) and KOH (1.009 g, 18 mmol) were stirred for 2 h in dry DMF (30 ml) and then 1-bromo-3-chloropropane (2.361 g, 15 mmol) was added to the mixture and stirred at room temperature for 24 h. Thereafter, the mixture was poured into ice/water and the separated solid was filtered off and washed with water then hexane to furnish the key intermediates **5a–c** which were used without further purification.

The spectral data of **5a,b** have been reported in our previous study³⁶.

4.1.5.1. 4-(3-chloropropoxy)-6,7-dimethoxy-2-(*p*-tolyl)quinoline (5c)

White solid, Yield 90%, m.p. 140–142 °C; ¹H NMR (400 MHz, CDCl₃) δ (ppm): 2.42 (s, 3H, CH₃), 2.43 (p, 2H, CH₂, *J* = 6.1 Hz), 3.83 (t, 2H, CH₂Cl, *J* = 6.2 Hz), 4.02 (s, 3H, OCH₃), 4.03 (s, 3H, OCH₃), 4.42 (t, 2H, CH₂-O, *J* = 6 Hz), 7.10 (s, 1H, vinyl CH), 7.30 (d, 2H, *p*-toluoyl 2CH, *J* = 8.1 Hz), 7.36 (s, 1H, phenyl CH), 7.44 (s, 1H, phenyl CH), 7.96 (d, 2H, *p*-toluoyl 2CH, *J* = 8.1 Hz); ¹³C NMR (100 MHz, CDCl₃) δ (ppm): 21.30, 32.01, 41.40, 56.05, 56.11, 64.81, 97.57, 99.58, 108.37, 114.64, 127.14, 129.43, 137.66, 138.87, 146.28, 148.88, 152.61, 156.97, 160.56; HRESIMS (*m/z*): [M + H]⁺ Calcd for C₂₁H₂₃ClNO₃, 372.13610; found, 372.13623.

4.1.6. General procedure for synthesis of the target 4-propoxy-2-arylquinolines (6a–o)

To a stirred mixture of **5a–c** (1 mmol), anhydrous K₂CO₃ (1.38 g, 10 mmol) and KI (0.83 g, 5 mmol) in dry DMF (20 ml), the respective amine (10 mmol) was added. Then, the mixture was refluxed at 90 °C for 12 h and poured into ice/water (50 ml). The separated solid was filtered off then washed with water and hexane. The products were purified by silica gel column chromatography using DCM/MeOH to furnish the pure target compounds **6a–o**.

4.1.6.1. 2-(4-chlorophenyl)-6,7-dimethoxy-4-(3-(4-methylpiperazin-1-yl)propoxy)quinoline (6a)

White solid, Yield 71%, m.p. 140–142 °C; ¹H NMR (400 MHz, CDCl₃) δ (ppm): 2.15 (p, 2H, CH₂, *J* = 6.8 Hz), 2.29 (s, 3H, CH₃-N), 2.36–2.66 (br s, 8H, piperazinyl 4CH₂), 2.62 (t, 2H, CH₂-N, *J* = 7.3 Hz), 4.01 (s, 3H, OCH₃), 4.02 (s, 3H, OCH₃), 4.31 (t, 2H, CH₂-O, *J* = 6.3 Hz), 7.03 (s, 1H, vinyl CH), 7.37 (s, 1H, phenyl CH), 7.40 (s, 1H, phenyl CH), 7.44 (d, 2H, chlorophenyl 2CH, *J* = 8.6 Hz), 7.99 (d, 2H, chlorophenyl 2CH, *J* = 8.6 Hz); ¹³C NMR (100 MHz, CDCl₃) δ (ppm): 26.59, 46.02, 53.31, 55.11, 56.04, 56.11, 66.65, 97.38, 99.68, 108.23, 114.93, 128.55, 128.82, 134.90, 139.00, 146.18, 149.07, 152.72, 155.59, 161.08; HRESIMS (*m/z*): [M + H]⁺ Calcd for C₂₅H₃₁ClN₃O₃, 456.20485; found, 456.20474; HPLC purity: 97.65%.

4.1.6.2. N-(3-((2-(4-chlorophenyl)-6,7-dimethoxyquinolin-4-yl)oxy)propyl)cyclohexanamine (6b)

Grey solid, Yield 80%, m.p. 118–120 °C; ¹H NMR (400 MHz, CDCl₃) δ (ppm): 1.02–1.13 (m, 2H, cyclohexyl 2CHH'), 1.14–1.19 (m, 1H, cyclohexyl CHH'), 1.20–1.30 (m, 2H, cyclohexyl 2CHH'), 1.44 (br s, 1H, NH), 1.59–1.63 (m, 1H, cyclohexyl CHH'), 1.70–1.74 (m, 2H, cyclohexyl 2CHH'), 1.89–1.92 (m, 2H, cyclohexyl 2CHH'), 2.14 (p, 2H, CH₂, *J* = 6.5 Hz), 2.43–2.50 (m, 1H, cyclohexyl CH-NH), 2.93 (t, 2H, CH₂-NH, *J* = 6.9 Hz), 4.02 (s, 3H, OCH₃), 4.03 (s, 3H, OCH₃), 4.35 (t, 2H, CH₂-O, *J* = 6.1 Hz), 7.06 (s, 1H, vinyl CH), 7.39 (s, 1H, phenyl CH), 7.41 (s, 1H, phenyl CH), 7.45 (d, 2H, chlorophenyl 2CH, *J* = 8.6 Hz), 8 (d, 2H, chlorophenyl 2CH, *J* = 8.6 Hz); ¹³C NMR (100 MHz, CDCl₃) δ (ppm): 25.06, 26.14,

30.00, 33.68, 43.90, 56.05, 56.12, 56.91, 66.94, 97.42, 99.67, 108.23, 114.94, 128.55, 128.82, 134.90, 138.98, 146.18, 149.07, 152.71, 155.61, 161.07; HRESIMS (*m/z*): [M + H]⁺ Calcd for C₂₆H₃₂ClN₂O₃, 455.20960; found, 455.20932; HPLC purity: 98.81%.

4.1.6.3. N-(3-((2-(4-chlorophenyl)-6,7-dimethoxyquinolin-4-yl)oxy)propyl)-1-methylpiperidin-4-amine (6c). White solid, Yield 70%, m.p. 124–126 °C; ¹H NMR (400 MHz, CDCl₃) δ (*ppm*): 1.35–1.45 (m, 3H, piperidiny 2CHH', NH), 1.89 (d, 2H, piperidiny 2CHH', *J* = 12.6 Hz), 1.97 (t, 2H, piperidiny 2CHH', *J* = 11.7 Hz), 2.14 (p, 2H, CH₂, *J* = 6.5 Hz), 2.25 (s, 3H, N-CH₃), 2.43–2.51 (m, 1H, piperidiny CH-NH), 2.80 (d, 2H, piperidiny 2CHH', *J* = 11.7 Hz), 2.92 (t, 2H, CH₂-NH, *J* = 6.9 Hz), 4.01 (s, 3H, OCH₃), 4.03 (s, 3H, OCH₃), 4.35 (t, 2H, CH₂-O, *J* = 6.1 Hz), 7.05 (s, 1H, vinyl CH), 7.37 (s, 1H, phenyl CH), 7.41 (s, 1H, phenyl CH), 7.44 (d, 2H, chlorophenyl 2CH, *J* = 8.6 Hz), 7.99 (d, 2H, chlorophenyl 2CH, *J* = 8.6 Hz); ¹³C NMR (100 MHz, CDCl₃) δ (*ppm*): 29.96, 32.91, 43.73, 46.23, 54.50, 54.64, 56.06, 56.12, 66.83, 97.39, 99.64, 108.25, 114.92, 128.54, 128.83, 134.91, 138.97, 146.19, 149.08, 152.72, 155.60, 161.05; HRESIMS (*m/z*): [M + H]⁺ Calcd for C₂₆H₃₃ClN₃O₃, 470.22050; found, 470.21988; HPLC purity: 96.18%.

4.1.6.4. 3-((2-(4-chlorophenyl)-6,7-dimethoxyquinolin-4-yl)oxy)-N-((tetrahydrofuran-2-yl)methyl)propan-1-amine (6d). White solid, Yield 74%, m.p. 108–110 °C; ¹H NMR (400 MHz, CDCl₃) δ (*ppm*): 1.48–1.57 (m, 1H, furyl CHH'), 1.66 (s, 1H, NH), 1.83–1.92 (m, 2H, furyl CH₂), 1.93–2 (m, 1H, furyl CHH'), 2.16 (p, 2H, CH₂, *J* = 6.6 Hz), 2.67 (dd, 1H, furfuryl CHH'-NH, *J* = 8, 12 Hz), 2.75 (dd, 1H, furfuryl CHH'-NH, *J* = 3.6, 12 Hz), 2.92 (t, 2H, CH₂-NH, *J* = 6.9 Hz), 3.70–3.75 (m, 1H, furyl CHH'-O), 3.80–3.85 (m, 1H, furyl CHH'-O), 4 (p, 1H, furyl CH-O, *J* = 3.6 Hz), 4.02 (s, 3H, OCH₃), 4.03 (s, 3H, OCH₃), 4.36 (t, 2H, CH₂-O, *J* = 6.2 Hz), 7.06 (s, 1H, vinyl CH), 7.39 (s, 1H, phenyl CH), 7.41 (s, 1H, phenyl CH), 7.44 (d, 2H, chlorophenyl 2CH, *J* = 8.6 Hz), 8 (d, 2H, chlorophenyl 2CH, *J* = 8.6 Hz); ¹³C NMR (100 MHz, CDCl₃) δ (*ppm*): 25.78, 29.32, 29.67, 46.99, 54.64, 56.08, 66.80, 67.95, 78.31, 97.41, 99.80, 108.25, 114.97, 128.55, 128.80, 134.88, 139.02, 146.20, 149.09, 152.73, 155.58, 161.12; HRESIMS (*m/z*): [M + H]⁺ Calcd for C₂₅H₃₀ClN₂O₄, 457.18886; found, 457.18936; HPLC purity: 97.34%.

4.1.6.5. 4-(3-(1H-imidazol-1-yl)propoxy)-2-(4-chlorophenyl)-6,7-dimethoxyquinoline (6e). White solid, Yield 75%, m.p. 209–211 °C; ¹H NMR (400 MHz, CDCl₃) δ (*ppm*): 2.43 (p, 2H, CH₂, *J* = 6.2 Hz), 4.03 (s, 3H, OCH₃), 4.04 (s, 3H, OCH₃), 4.22 (t, 2H, CH₂-N, *J* = 5.8 Hz), 4.28 (t, 2H, CH₂-O, *J* = 6.6 Hz), 6.94 (s, 1H, imidazole CH), 6.96 (s, 1H, vinyl CH), 7.07 (s, 1H, imidazole CH), 7.33 (s, 1H, phenyl CH), 7.43 (s, 1H, phenyl CH), 7.44 (d, 2H, chlorophenyl 2CH, *J* = 8.5 Hz), 7.50 (s, 1H, imidazole CH), 7.96 (d, 2H, chlorophenyl 2CH, *J* = 8.5 Hz); ¹³C NMR (100 MHz, CDCl₃) δ (*ppm*): 30.51, 43.59, 56.12, 64.48, 97.30, 99.33, 108.44, 114.67, 118.87, 128.51, 128.85, 130.03, 135.05, 137.23, 138.73, 146.34, 149.36, 152.94, 155.55, 160.43; HRESIMS (*m/z*): [M + H]⁺ Calcd for C₂₃H₂₃ClN₃O₃, 424.14225; found, 424.14264; HPLC purity: 99.50%.

4.1.6.6. 6,7-dimethoxy-4-(3-(4-methylpiperazin-1-yl)propoxy)-2-(4-(trifluoromethyl)phenyl)quinoline (6f). White solid, Yield 71%, m.p. 84–86 °C; ¹H NMR (400 MHz, CDCl₃) δ (*ppm*): 2.17 (p, 2H, CH₂, *J* = 6.8 Hz), 2.29 (s, 3H, CH₃-N), 2.36–2.71 (br s, 8H, piperazinyl 4CH₂), 2.63 (t, 2H, CH₂-N, *J* = 7.3 Hz), 4.02 (s, 3H, OCH₃), 4.03 (s, 3H, OCH₃), 4.33 (t, 2H, CH₂-O, *J* = 6.3 Hz), 7.09 (s, 1H, vinyl CH), 7.39 (s, 1H, phenyl CH), 7.43 (s, 1H, phenyl CH), 7.73 (d, 2H, CF₃-phenyl 2CH, *J* = 8.2 Hz), 8.16 (d, 2H, CF₃-phenyl 2CH, *J* = 8.2 Hz); ¹³C NMR

(100 MHz, CDCl₃) δ (*ppm*): 26.59, 46.03, 53.34, 55.12, 56.07, 56.13, 66.72, 97.71, 99.64, 108.28, 115.18, 124.26 (CF₃, q, *J* = 271.7 Hz), 125.59 (CH-C-CF₃, q, *J* = 3.9 Hz), 127.59, 130.59 (CH-C-CF₃, q, *J* = 32.4 Hz), 143.94, 146.24, 149.32, 152.84, 155.25, 161.18; ¹⁹F NMR (376.46 MHz, CDCl₃) δ (*ppm*): -62.47 (s); HRESIMS (*m/z*): [M + H]⁺ Calcd for C₂₆H₃₁F₃N₃O₃, 490.23120; found, 490.23087; HPLC purity: 98.93%.

4.1.6.7. N-(3-((6,7-dimethoxy-2-(4-(trifluoromethyl)phenyl)quinolin-4-yl)oxy)propyl)cyclohexan-amine (6g). Grey solid, Yield 75%, m.p. 131–133 °C; ¹H NMR (400 MHz, CDCl₃) δ (*ppm*): 1.02–1.12 (m, 2H, cyclohexyl 2CHH'), 1.13–1.19 (m, 1H, cyclohexyl CHH'), 1.20–1.30 (m, 2H, cyclohexyl 2CHH'), 1.37 (br s, 1H, NH), 1.59–1.63 (m, 1H, cyclohexyl CHH'), 1.70–1.74 (m, 2H, cyclohexyl 2CHH'), 1.89–1.92 (m, 2H, cyclohexyl 2CHH'), 2.15 (p, 2H, CH₂, *J* = 6.5 Hz), 2.43–2.50 (m, 1H, cyclohexyl CH-NH), 2.93 (t, 2H, CH₂-NH, *J* = 6.9 Hz), 4.03 (s, 3H, OCH₃), 4.04 (s, 3H, OCH₃), 4.37 (t, 2H, CH₂-O, *J* = 6.1 Hz), 7.11 (s, 1H, vinyl CH), 7.40 (s, 1H, phenyl CH), 7.43 (s, 1H, phenyl CH), 7.73 (d, 2H, CF₃-phenyl 2CH, *J* = 8.2 Hz), 8.16 (d, 2H, CF₃-phenyl 2CH, *J* = 8.2 Hz); ¹³C NMR (100 MHz, CDCl₃) δ (*ppm*): 25.05, 26.14, 30.03, 33.71, 43.87, 56.07, 56.13, 56.90, 67.01, 97.73, 99.64, 108.30, 115.19, 124.26 (CF₃, q, *J* = 272 Hz), 125.59 (CH-C-CF₃, q, *J* = 3.7 Hz), 127.57, 130.62 (CH-C-CF₃, q, *J* = 33.9 Hz), 143.92, 146.24, 149.33, 152.84, 155.25, 161.17; ¹⁹F NMR (376.46 MHz, CDCl₃) δ (*ppm*): -62.47 (s); HRESIMS (*m/z*): [M + H]⁺ Calcd for C₂₇H₃₂F₃N₂O₃, 489.23595; found 489.23578; HPLC purity: 99.37%.

4.1.6.8. N-(3-((6,7-dimethoxy-2-(4-(trifluoromethyl)phenyl)quinolin-4-yl)oxy)propyl)-1-methyl piperidin-4-amine (6h). White solid, Yield 78%, m.p. 137–139 °C; ¹H NMR (400 MHz, CDCl₃) δ (*ppm*): 1.36–1.45 (m, 3H, piperidiny 2CHH', NH), 1.89 (d, 2H, piperidiny 2CHH', *J* = 12.5 Hz), 1.97 (t, 2H, piperidiny 2CHH', *J* = 11.7 Hz), 2.14 (p, 2H, CH₂, *J* = 6.5 Hz), 2.25 (s, 3H, N-CH₃), 2.43–2.51 (m, 1H, piperidiny CH-NH), 2.80 (d, 2H, piperidiny 2CHH', *J* = 11.7 Hz), 2.92 (t, 2H, CH₂-NH, *J* = 6.9 Hz), 4.02 (s, 3H, OCH₃), 4.04 (s, 3H, OCH₃), 4.37 (t, 2H, CH₂-O, *J* = 6.1 Hz), 7.10 (s, 1H, vinyl CH), 7.39 (s, 1H, phenyl CH), 7.43 (s, 1H, phenyl CH), 7.73 (d, 2H, CF₃-phenyl 2CH, *J* = 8.2 Hz), 8.16 (d, 2H, CF₃-phenyl 2CH, *J* = 8.2 Hz); ¹³C NMR (100 MHz, CDCl₃) δ (*ppm*): 29.95, 32.89, 43.68, 46.21, 54.50, 54.63, 56.08, 56.14, 66.89, 97.71, 99.61, 108.31, 115.17, 124.27 (CF₃, q, *J* = 272.6 Hz), 125.60 (CH-C-CF₃, q, *J* = 3.9 Hz), 127.57, 130.64 (CH-C-CF₃, q, *J* = 32.7 Hz), 143.90, 146.25, 149.34, 152.85, 155.26, 161.15; ¹⁹F NMR (376.46 MHz, CDCl₃) δ (*ppm*): -62.47 (s); HRESIMS (*m/z*): [M + H]⁺ Calcd for C₂₇H₃₃F₃N₃O₃, 504.24685; found, 504.24692; HPLC purity: 99.75%.

4.1.6.9. 3-((6,7-dimethoxy-2-(4-(trifluoromethyl)phenyl)quinolin-4-yl)oxy)-N-((tetrahydrofuran-2-yl)methyl)propan-1-amine (6i). White solid, Yield 76%, m.p. 105–107 °C; ¹H NMR (400 MHz, CDCl₃) δ (*ppm*): 1.49–1.57 (m, 1H, furyl CHH'), 1.69 (s, 1H, NH), 1.83–1.92 (m, 2H, furyl CH₂), 1.93–2 (m, 1H, furyl CHH'), 2.18 (p, 2H, CH₂, *J* = 6.6 Hz), 2.68 (dd, 1H, furfuryl CHH'-NH, *J* = 8, 12 Hz), 2.75 (dd, 1H, furfuryl CHH'-NH, *J* = 3.5, 12 Hz), 2.93 (t, 2H, CH₂-NH, *J* = 6.9 Hz), 3.70–3.75 (m, 1H, furyl CHH'-O), 3.80–3.86 (m, 1H, furyl CHH'-O), 4 (p, 1H, furyl CH-O, *J* = 3.5 Hz), 4.03 (s, 3H, OCH₃), 4.04 (s, 3H, OCH₃), 4.38 (t, 2H, CH₂-O, *J* = 6.2 Hz), 7.11 (s, 1H, vinyl CH), 7.41 (s, 1H, phenyl CH), 7.43 (s, 1H, phenyl CH), 7.43 (d, 2H, CF₃-phenyl 2CH, *J* = 8.2 Hz), 8.16 (d, 2H, chlorophenyl 2CH, *J* = 8.2 Hz); ¹³C NMR (100 MHz, CDCl₃) δ (*ppm*): 25.78, 29.32, 29.64, 47.00, 54.67, 56.11, 56.13, 66.87, 67.97, 78.28, 97.74, 99.72, 108.26, 115.20, 124.28 (CF₃, q, *J* = 272 Hz), 125.58 (CH-C-CF₃, q, *J* = 3.8 Hz), 127.58, 130.59 (CH-C-CF₃, q, *J* = 32.3 Hz), 143.92, 146.23, 149.31,

152.82, 155.24, 161.20; ^{19}F NMR (376.46 MHz, CDCl_3) δ (ppm): -62.46 (s); HRESIMS (m/z): $[\text{M} + \text{H}]^+$ Calcd for $\text{C}_{26}\text{H}_{30}\text{F}_3\text{N}_2\text{O}_4$, 491.21522; found, 491.21533; HPLC purity: 99.63%.

4.1.6.10. 4-(3-(1H-imidazol-1-yl)propoxy)-6,7-dimethoxy-2-(4-(trifluoromethyl)phenyl)quinoline (6j). White solid, Yield 88%, m.p. 217–219 °C; ^1H NMR (400 MHz, CDCl_3) δ (ppm): 2.45 (p, 2H, CH_2 , $J = 6.2$ Hz), 4.05 (s, 3H, OCH_3), 4.06 (s, 3H, OCH_3), 4.24 (t, 2H, $\text{CH}_2\text{-N}$, $J = 5.8$ Hz), 4.29 (t, 2H, $\text{CH}_2\text{-O}$, $J = 6.6$ Hz), 6.94 (s, 1H, imidazole CH), 7.01 (s, 1H, vinyl CH), 7.08 (s, 1H, imidazole CH), 7.35 (s, 1H, phenyl CH), 7.46 (s, 1H, phenyl CH), 7.51 (s, 1H, imidazole CH), 7.73 (d, 2H, CF_3 -phenyl 2CH, $J = 8.2$ Hz), 8.13 (d, 2H, CF_3 -phenyl 2CH, $J = 8.2$ Hz); ^{13}C NMR (100 MHz, CDCl_3) δ (ppm): 30.49, 43.58, 56.15, 56.18, 64.54, 97.63, 99.24, 108.47, 114.90, 118.88, 124.23 (CF_3 , q, $J = 272$ Hz), 125.63 (CH-C-F_3 , q, $J = 3.7$ Hz), 127.56, 130.05, 130.72 (CH-C-F_3 , q, $J = 32.5$ Hz), 137.25, 143.64, 146.38, 149.59, 153.03, 155.22, 160.51; ^{19}F NMR (376.46 MHz, CDCl_3) δ (ppm): -62.48 (s); HRESIMS (m/z): $[\text{M} + \text{H}]^+$ Calcd for $\text{C}_{24}\text{H}_{23}\text{F}_3\text{N}_3\text{O}_3$, 458.16860; found, 458.16879; HPLC purity: 99.78%.

4.1.6.11. 6,7-dimethoxy-4-(3-(4-methylpiperazin-1-yl)propoxy)-2-(p-tolyl)quinoline (6k). White solid, Yield 70%, m.p. 128–130 °C; ^1H NMR (400 MHz, CDCl_3) δ (ppm): 2.15 (p, 2H, CH_2 , $J = 6.8$ Hz), 2.29 (s, 3H, $\text{CH}_3\text{-N}$), 2.41 (s, 3H, tolyl CH_3), 2.41–2.64 (br s, 8H, piperazinyl 4 CH_2), 2.62 (t, 2H, $\text{CH}_2\text{-N}$, $J = 7.3$ Hz), 4.01 (s, 3H, OCH_3), 4.02 (s, 3H, OCH_3), 4.31 (t, 2H, $\text{CH}_2\text{-O}$, $J = 6.3$ Hz), 7.07 (s, 1H, vinyl CH), 7.44 (d, 2H, tolyl 2CH, $J = 8$ Hz), 7.38 (s, 1H, phenyl CH), 7.43 (s, 1H, phenyl CH), 7.94 (d, 2H, tolyl 2CH, $J = 8$ Hz); ^{13}C NMR (100 MHz, CDCl_3) δ (ppm): 21.29, 26.62, 46.03, 53.33, 55.12, 55.17, 56.02, 56.09, 66.56, 97.58, 99.72, 108.30, 114.76, 127.16, 129.39, 137.79, 138.77, 146.20, 148.77, 152.52, 157.01, 160.91; HRESIMS (m/z): $[\text{M} + \text{H}]^+$ Calcd for $\text{C}_{26}\text{H}_{34}\text{N}_3\text{O}_3$, 436.25947; found, 436.25943; HPLC purity: 96.05%.

4.1.6.12. N-(3-((6,7-dimethoxy-2-(p-tolyl)quinolin-4-yl)oxy)propyl)-cyclohexanamine (6l). Buff solid, Yield 73%, m.p. 126–128 °C; ^1H NMR (400 MHz, CDCl_3) δ (ppm): 1.03–1.14 (m, 2H, cyclohexyl 2 CHH'), 1.15–1.21 (m, 1H, cyclohexyl CHH'), 1.23–1.30 (m, 2H, cyclohexyl 2 CHH'), 1.59–1.63 (m, 2H, cyclohexyl CHH' , NH), 1.70–1.75 (m, 2H, cyclohexyl 2 CHH'), 1.89–1.93 (m, 2H, cyclohexyl 2 CHH'), 2.15 (p, 2H, CH_2 , $J = 6.6$ Hz), 2.41 (s, 3H, tolyl CH_3), 2.44–2.51 (m, 1H, cyclohexyl CH-NH), 2.93 (t, 2H, $\text{CH}_2\text{-NH}$, $J = 7$ Hz), 4.01 (s, 3H, OCH_3), 4.03 (s, 3H, OCH_3), 4.34 (t, 2H, $\text{CH}_2\text{-O}$, $J = 6.1$ Hz), 7.08 (s, 1H, vinyl CH), 7.29 (d, 2H, tolyl 2CH, $J = 8$ Hz), 7.39 (s, 1H, phenyl CH), 7.43 (s, 1H, phenyl CH), 7.95 (d, 2H, tolyl 2CH, $J = 8$ Hz); ^{13}C NMR (100 MHz, CDCl_3) δ (ppm): 21.29, 25.05, 26.13, 29.96, 33.62, 43.93, 56.03, 56.09, 56.91, 66.84, 97.60, 99.71, 108.32, 114.77, 127.15, 129.40, 137.77, 138.78, 146.21, 148.79, 152.52, 157.01, 160.88; HRESIMS (m/z): $[\text{M} + \text{H}]^+$ Calcd for $\text{C}_{27}\text{H}_{35}\text{N}_2\text{O}_3$, 435.26422; found, 435.26422; HPLC purity: 97.90%.

4.1.6.13. N-(3-((6,7-dimethoxy-2-(p-tolyl)quinolin-4-yl)oxy)propyl)-1-methylpiperidin-4-amine (6m). White solid, Yield 76%, m.p. 66–68 °C; ^1H NMR (400 MHz, CDCl_3) δ (ppm): 1.35–1.45 (m, 3H, piperidinyl 2 CHH' , NH), 1.89 (d, 2H, piperidinyl 2 CHH' , $J = 12.5$ Hz), 1.96 (t, 2H, piperidinyl 2 CHH' , $J = 11.8$ Hz), 2.13 (p, 2H, CH_2 , $J = 6.5$ Hz), 2.24 (s, 3H, N- CH_3), 2.41 (s, 3H, tolyl CH_3), 2.43–2.50 (m, 1H, piperidinyl CH-NH), 2.80 (d, 2H, piperidinyl 2 CHH' , $J = 11.8$ Hz), 2.91 (t, 2H, $\text{CH}_2\text{-NH}$, $J = 6.9$ Hz), 4.01 (s, 3H, OCH_3), 4.02 (s, 3H, OCH_3), 4.34 (t, 2H, $\text{CH}_2\text{-O}$, $J = 6.1$ Hz), 7.08 (s, 1H, vinyl CH), 7.28 (d, 2H, tolyl 2CH, $J = 8$ Hz), 7.37 (s, 1H, phenyl CH), 7.43 (s, 1H, phenyl CH), 7.94 (d, 2H, tolyl 2CH, $J = 8$ Hz); ^{13}C NMR (100 MHz, CDCl_3) δ (ppm): 21.29, 29.97, 32.90, 43.79, 46.22, 54.49, 54.64, 56.03, 56.09,

66.74, 97.58, 99.68, 108.33, 114.75, 127.14, 129.40, 137.76, 138.79, 146.21, 148.79, 152.53, 157.00, 160.87; HRESIMS (m/z): $[\text{M} + \text{H}]^+$ Calcd for $\text{C}_{27}\text{H}_{36}\text{N}_3\text{O}_3$, 450.27512; found, 450.27481; HPLC purity: 95.52%.

4.1.6.14. 3-((6,7-dimethoxy-2-(p-tolyl)quinolin-4-yl)oxy)-N-((tetrahydrofuran-2-yl)methyl)propa- n-1-amine (6n). Yellow solid, Yield 85%, m.p. 60–62 °C; ^1H NMR (400 MHz, CDCl_3) δ (ppm): 1.48–1.57 (m, 1H, furyl CHH'), 1.83–2.00 (m, 4H, furyl CH_2 , furyl CHH' , NH), 2.16 (p, 2H, CH_2 , $J = 6.5$ Hz), 2.41 (s, 3H, tolyl CH_3), 2.67 (dd, 1H, furfuryl $\text{CHH}'\text{-NH}$, $J = 8$, 12 Hz), 2.74 (dd, 1H, furfuryl $\text{CHH}'\text{-NH}$, $J = 3.6$, 12 Hz), 2.92 (t, 2H, $\text{CH}_2\text{-NH}$, $J = 6.8$ Hz), 3.69–3.75 (m, 1H, furyl $\text{CHH}'\text{-O}$), 3.79–3.85 (m, 1H, furyl $\text{CHH}'\text{-O}$), 4 (p, 1H, furyl CH-O , $J = 3.6$ Hz), 4.02 (s, 3H, OCH_3), 4.03 (s, 3H, OCH_3), 4.35 (t, 2H, $\text{CH}_2\text{-O}$, $J = 6.2$ Hz), 7.08 (s, 1H, vinyl CH), 7.29 (d, 2H, tolyl 2CH, $J = 8$ Hz), 7.39 (s, 1H, phenyl CH), 7.43 (s, 1H, phenyl CH), 7.94 (d, 2H, tolyl 2CH, $J = 8$ Hz); ^{13}C NMR (100 MHz, CDCl_3) δ (ppm): 21.28, 25.77, 29.33, 29.61, 47.06, 54.61, 56.06, 56.08, 66.70, 67.95, 78.23, 97.64, 99.80, 108.22, 114.78, 127.18, 129.39, 137.76, 138.78, 146.16, 148.78, 152.53, 157.03, 160.93; HRESIMS (m/z): $[\text{M} + \text{H}]^+$ Calcd for $\text{C}_{26}\text{H}_{33}\text{N}_2\text{O}_4$, 437.24348; found, 437.24353; HPLC purity: 97.50%.

4.1.6.15. 4-(3-(1H-imidazol-1-yl)propoxy)-6,7-dimethoxy-2-(p-tolyl)quinoline (6o). White solid, Yield 83%, m.p. 203–205 °C; ^1H NMR (400 MHz, CDCl_3) δ (ppm): 2.41 (s, 3H, tolyl CH_3), 2.42 (p, 2H, CH_2 , $J = 6.3$ Hz), 4.03 (s, 6H, 2 CH_3O), 4.22 (t, 2H, $\text{CH}_2\text{-N}$, $J = 5.8$ Hz), 4.27 (t, 2H, $\text{CH}_2\text{-O}$, $J = 6.7$ Hz), 6.93 (s, 1H, imidazole CH), 6.99 (s, 1H, vinyl CH), 7.07 (s, 1H, imidazole CH), 7.28 (d, 2H, tolyl 2CH, $J = 8.1$ Hz), 7.34 (s, 1H, phenyl CH), 7.45 (s, 1H, phenyl CH), 7.51 (s, 1H, imidazole CH), 7.92 (d, 2H, tolyl 2CH, $J = 8.1$ Hz); ^{13}C NMR (100 MHz, CDCl_3) δ (ppm): 21.29, 30.55, 43.62, 56.10, 56.13, 64.37, 97.50, 99.35, 108.48, 114.48, 118.92, 127.12, 129.44, 129.97, 137.22, 137.51, 138.96, 146.34, 149.03, 152.71, 156.97, 160.25; HRESIMS (m/z): $[\text{M} + \text{H}]^+$ Calcd for $\text{C}_{24}\text{H}_{26}\text{N}_3\text{O}_3$, 404.19687; found, 404.19724; HPLC purity: 99.42%.

4.1.7. Synthesis of 2-(4-bromophenyl)-6,7-dimethoxy-4-(3-(4-methylpiperazin-1-yl)propoxy)quinoline (7)

The bromo analog of 4-propoxy-N-methylpiperazine-2-arylquinoline **7** has been prepared using the same synthetic procedure as **6a–o** utilising *p*-bromobenzoyl chloride.

White solid, Yield 77%, m.p. 148–150 °C; ^1H NMR (400 MHz, CDCl_3) δ (ppm): 2.15 (p, 2H, CH_2 , $J = 6.8$ Hz), 2.29 (s, 3H, $\text{CH}_3\text{-N}$), 2.36–2.66 (br s, 8H, piperazinyl 4 CH_2), 2.62 (t, 2H, $\text{CH}_2\text{-N}$, $J = 7.3$ Hz), 4.01 (s, 3H, OCH_3), 4.02 (s, 3H, OCH_3), 4.31 (t, 2H, $\text{CH}_2\text{-O}$, $J = 6.3$ Hz), 7.03 (s, 1H, vinyl CH), 7.37 (s, 1H, phenyl CH), 7.41 (s, 1H, phenyl CH), 7.60 (d, 2H, bromophenyl 2CH, $J = 8.6$ Hz), 7.92 (d, 2H, bromophenyl 2CH, $J = 8.6$ Hz); ^{13}C NMR (100 MHz, CDCl_3) δ (ppm): 26.57, 45.96, 53.24, 55.07, 56.04, 56.10, 66.65, 97.34, 99.71, 108.23, 114.97, 123.23, 128.85, 131.77, 139.45, 146.20, 149.11, 152.76, 155.62, 161.10; HRESIMS (m/z): $[\text{M} + \text{H}]^+$ Calcd for $\text{C}_{25}\text{H}_{31}\text{BrN}_3\text{O}_3$, 500.15433; found, 500.15466.

4.1.8. General procedure for synthesis of heterocyclic analogs of the bromo derivative (8a,b)

The bromo derivative **7** (125 mg, 0.25 mmol) was taken with 2-furylboronic acid or 2-thienylboronic acid (0.5 mmol) and $\text{Pd}(\text{PPh}_3)_4$ (0.05 equivalent, 15 mg), then dioxane (5 ml) and 2 M Na_2CO_3 (0.3 ml) were added to the mixture under N_2 atmosphere. The reaction mixture was refluxed under N_2 at 90 °C for 16 h. Then, the reaction mixture was poured into ice/water (50 ml), the

aqueous layer was extracted with ethyl acetate (50 × 3) and the organic layers were washed with water and brine. After evaporation of the organic solvent under vacuum, the residue was purified by silica gel column chromatography using DCM/MeOH to furnish **8a,b** in pure form.

4.1.8.1. 2-(4-(furan-2-yl)phenyl)-6,7-dimethoxy-4-(3-(4-methylpiperazin-1-yl)propoxy)quinoline (8a). Yellow solid, Yield 70%, m.p. 135–137 °C; ¹H NMR (400 MHz, CDCl₃) δ (ppm): 2.17 (p, 2H, CH₂, J = 6.8 Hz), 2.34 (s, 3H, CH₃-N), 2.43–2.78 (br s, 8H, piperazinyl 4CH₂), 2.66 (t, 2H, CH₂-N, J = 7.3 Hz), 4.02 (s, 3H, OCH₃), 4.04 (s, 3H, OCH₃), 4.33 (t, 2H, CH₂-O, J = 6.3 Hz), 6.50 (dd, 1H, furyl CH, J = 1.8, 3.4 Hz), 6.73 (dd, 1H, furyl CH, J = 0.5, 3.4 Hz), 7.11 (s, 1H, vinyl CH), 7.38 (s, 1H, phenyl CH), 7.44 (s, 1H, phenyl CH), 7.50 (dd, 1H, furyl CH-O, J = 0.5, 1.8 Hz), 7.79 (d, 2H, 2-phenyl 2CH, J = 8.5 Hz), 8.09 (d, 2H, 2-phenyl 2CH, J = 8.5 Hz); ¹³C NMR (100 MHz, CDCl₃) δ (ppm): 26.53, 45.73, 52.86, 54.91, 55.02, 56.07, 56.12, 66.51, 97.49, 99.69, 105.63, 108.28, 111.83, 114.89, 124.02, 127.58, 131.21, 139.24, 142.35, 146.23, 148.95, 152.65, 153.71, 156.27, 160.95; HRESIMS (m/z): [M + H]⁺ Calcd for C₂₉H₃₄N₃O₄, 488.25438; found, 488.25446; HPLC purity: 96.06%.

4.1.8.2. 6,7-dimethoxy-4-(3-(4-methylpiperazin-1-yl)propoxy)-2-(4-(thiophen-2-yl)phenyl)quinoline (8b). Buff solid, Yield 72%, m.p. 155–157 °C; ¹H NMR (400 MHz, CDCl₃) δ (ppm): 2.17 (p, 2H, CH₂, J = 6.8 Hz), 2.29 (s, 3H, CH₃-N), 2.34–2.70 (br s, 8H, piperazinyl 4CH₂), 2.63 (t, 2H, CH₂-N, J = 7.3 Hz), 4.02 (s, 3H, OCH₃), 4.03 (s, 3H, OCH₃), 4.33 (t, 2H, CH₂-O, J = 6.3 Hz), 7.09 (dd, 1H, thienyl CH, J = 3.7, 5.1 Hz), 7.10 (s, 1H, vinyl CH), 7.30 (dd, 1H, thienyl CH, J = 1.1, 5.1 Hz), 7.38 (dd, 1H, thienyl CH-S, J = 1.1, 3.7 Hz), 7.39 (s, 1H, phenyl CH), 7.44 (s, 1H, phenyl CH), 7.73 (d, 2H, 2-phenyl 2CH, J = 8.4 Hz), 8.08 (d, 2H, 2-phenyl 2CH, J = 8.4 Hz); ¹³C NMR (100 MHz, CDCl₃) δ (ppm): 26.62, 46.05, 53.35, 55.13, 55.17, 56.04, 56.12, 66.62, 97.49, 99.72, 108.30, 114.94, 123.39, 125.12, 126.09, 127.76, 128.13, 134.80, 139.52, 144.01, 146.25, 148.95, 152.64, 156.20, 160.99; HRESIMS (m/z): [M + H]⁺ Calcd for C₂₉H₃₄N₃O₃S, 504.23154; found, 504.23141; HPLC purity: 98.96%.

4.1.9. Synthesis of 4-(3-chloropropoxy)-2-(4-(trifluoromethyl)phenyl)quinoline (9)

The demethoxylated key intermediate **9** has been synthesised using the same synthetic procedure for **5a–c** starting from 2-aminoacetophenone.

White solid, Yield 76%, m.p. 98–100 °C; ¹H NMR (400 MHz, CDCl₃) δ (ppm): 2.45 (p, 2H, CH₂, J = 6 Hz), 2.87 (t, 2H, CH₂-N, J = 6.2 Hz), 4.46 (t, 2H, CH₂-O, J = 5.8 Hz), 7.20 (s, 1H, vinyl CH), 7.52 (ddd, 1H, phenyl CH, J = 1.2, 6.9, 8.3 Hz), 7.74 (ddd, 1H, phenyl CH, J = 1.3, 6.9, 8.4 Hz), 7.77 (d, 2H, CF₃-phenyl 2CH, J = 8.2 Hz), 8.11 (d, 2H, phenyl CH, J = 8.4 Hz), 8.19 (dd, 1H, phenyl CH, J = 1.3, 8.3 Hz), 8.22 (d, 2H, CF₃-phenyl 2CH, J = 8.2 Hz); ¹³C NMR (100 MHz, CDCl₃) δ (ppm): 31.94, 41.23, 64.86, 98.50, 121.56, 124.20 (CF₃, q, J = 272 Hz), 125.67 (CH-C-CF₃, q, J = 3.7 Hz), 125.96, 127.87, 129.42, 130.31, 131.08 (CH-C-CF₃, q, J = 32.4 Hz), 143.56, 149.23, 157.12, 162.07; ¹⁹F NMR (376.46 MHz, CDCl₃) δ (ppm): -62.53 (s); HRESIMS (m/z): [M + H]⁺ Calcd for C₁₉H₁₆ClF₃NO, 366.08670; found, 366.08725.

4.1.10. Synthesis of the target demethoxylated 4-propoxy-2-arylquinolines (10a,b)

The demethoxylated 4-propoxy-2-arylquinolines **10a,b** were prepared according to the general synthetic procedure for **6a–o** using the respective key intermediate **9**.

4.1.10.1. 4-(3-(4-methylpiperazin-1-yl)propoxy)-2-(4-(trifluoromethyl)phenyl)quinoline (10a). White solid, Yield 87%, m.p. 110–112 °C; ¹H NMR (400 MHz, CDCl₃) δ (ppm): 2.16 (p, 2H, CH₂, J = 6.7 Hz), 2.29 (s, 3H, CH₃-N), 2.37–2.71 (br s, 8H, piperazinyl 4CH₂), 2.64 (t, 2H, CH₂-N, J = 7.2 Hz), 4.34 (t, 2H, CH₂-O, J = 6.2 Hz), 7.16 (s, 1H, vinyl CH), 7.50 (ddd, 1H, phenyl CH, J = 1.1, 6.9, 8.2 Hz), 7.72 (ddd, 1H, phenyl CH, J = 1.5, 6.9, 8.3 Hz), 7.75 (d, 2H, CF₃-phenyl 2CH, J = 8.2 Hz), 8.09 (d, 2H, phenyl CH, J = 8.3 Hz), 8.2 (m, 3H, phenyl CH, CF₃-phenyl 2CH); ¹³C NMR (100 MHz, CDCl₃) δ (ppm): 26.54, 46.04, 53.30, 55.00, 55.13, 66.79, 98.49, 120.63, 121.74, 124.21 (CF₃, q, J = 272 Hz), 125.63 (CH-C-CF₃, q, J = 3.8 Hz), 125.82, 127.89, 129.32, 130.21, 130.99 (CH-C-CF₃, q, J = 32.6 Hz), 143.72, 149.19, 157.14, 162.43; ¹⁹F NMR (376.46 MHz, CDCl₃) δ (ppm): -62.53 (s); HRESIMS (m/z): [M + Na]⁺ Calcd for C₂₁H₃₃ClF₃NONa, 430.20950; found, 430.20993; HPLC purity: 98.63%.

4.1.10.2. N-(3-((2-(4-(trifluoromethyl)phenyl)quinolin-4-yl)oxy)propyl)cyclohexanamine (10b). Grey solid, Yield 78%, m.p. 68–70 °C; ¹H NMR (400 MHz, CDCl₃) δ (ppm): 1.03–1.13 (m, 2H, cyclohexyl 2CHH'), 1.14–1.19 (m, 1H, cyclohexyl CHH'), 1.20–1.31 (m, 3H, cyclohexyl 2CHH', NH), 1.60–1.63 (m, 1H, cyclohexyl CHH'), 1.71–1.75 (m, 2H, cyclohexyl 2CHH'), 1.91 (d, 2H, cyclohexyl 2CHH', J = 10.2 Hz), 2.15 (p, 2H, CH₂, J = 6.5 Hz), 2.43–2.50 (m, 1H, cyclohexyl CH-NH), 2.94 (t, 2H, CH₂-NH, J = 6.9 Hz), 4.38 (t, 2H, CH₂-O, J = 6.1 Hz), 7.18 (s, 1H, vinyl CH), 7.51 (ddd, 1H, phenyl CH, J = 1.1, 7, 8.1 Hz), 7.72 (ddd, 1H, phenyl CH, J = 1.4, 7, 8.3 Hz), 7.75 (d, 2H, CF₃-phenyl 2CH, J = 8.7 Hz), 8.09 (d, 2H, phenyl CH, J = 8.3 Hz), 8.21 (d, 3H, phenyl CH, CF₃-phenyl 2CH, J = 8.1 Hz); ¹³C NMR (100 MHz, CDCl₃) δ (ppm): 25.08, 26.16, 30.05, 33.71, 43.77, 56.94, 67.04, 98.51, 120.64, 121.74, 124.25 (CF₃, q, J = 271.7 Hz), 125.64 (CH-C-CF₃, q, J = 3.7 Hz), 125.82, 127.88, 129.33, 130.20, 130.99 (CH-C-CF₃, q, J = 32.4 Hz), 143.70, 149.20, 157.15, 162.42; ¹⁹F NMR (376.46 MHz, CDCl₃) δ (ppm): -62.53 (s); HRESIMS (m/z): [M + H]⁺ Calcd for C₂₅H₂₈F₃N₂O, 429.21482; found, 429.21420; HPLC purity: 99.22%.

4.1.11. Synthesis of 1,3-dioxoloarylquinolines key intermediates (11a,b)

Starting from 6'-amino-3',4'-(methylenedioxy)acetophenone and the respective *p*-substituted benzoyl chloride, the key intermediates **11a,b** were prepared according to the synthetic route for **5a–c**.

4.1.11.1. 6-(4-chlorophenyl)-8-(3-chloropropoxy)-[1,3]dioxolo[4,5-g]quinoline (11a). White solid, Yield 90%, m.p. 186–188 °C; ¹H NMR (400 MHz, CDCl₃) δ (ppm): 2.40 (p, 2H, CH₂, J = 6 Hz), 3.83 (t, 2H, CH₂Cl, J = 6.2 Hz), 4.39 (t, 2H, CH₂-O, J = 5.8 Hz), 6.09 (s, 2H, dioxolo CH₂), 7.05 (s, 1H, vinyl CH), 7.37 (s, 1H, phenyl CH), 7.39 (s, 1H, phenyl CH), 7.45 (d, 2H, chlorophenyl 2CH, J = 8.6 Hz), 8 (d, 2H, chlorophenyl 2CH, J = 8.6 Hz); ¹³C NMR (100 MHz, CDCl₃) δ (ppm): 31.99, 41.27, 64.68, 97.50, 101.68, 106.01, 116.23, 128.53, 128.84, 135.06, 138.63, 147.30, 147.48, 151.04, 155.48, 161.15; HRESIMS (m/z): [M + H]⁺ Calcd for C₁₉H₁₆Cl₂NO₃, 376.05018; found, 376.05045.

4.1.11.2. 8-(3-chloropropoxy)-6-(4-(trifluoromethyl)phenyl)-[1,3]dioxolo[4,5-g]quinoline (11b). White solid, Yield 93%, m.p. 145–147 °C; ¹H NMR (400 MHz, CDCl₃) δ (ppm): 2.41 (p, 2H, CH₂, J = 6 Hz), 3.84 (t, 2H, CH₂Cl, J = 6.2 Hz), 4.41 (t, 2H, CH₂-O, J = 5.8 Hz), 6.10 (s, 2H, dioxolo CH₂), 7.10 (s, 1H, vinyl CH), 7.39 (s, 1H, phenyl CH), 7.40 (s, 1H, phenyl CH), 7.73 (d, 2H, CF₃-phenyl

2CH, $J = 8.1$ Hz), 8.16 (d, 2H, CF₃-phenyl 2CH, $J = 8.1$ Hz); ¹³C NMR (100 MHz, CDCl₃) δ (ppm): 31.96, 41.24, 64.74, 97.50, 97.83, 101.75, 106.09, 116.50, 124.25 (CF₃, q, $J = 271.8$ Hz), 125.61 (CH-C-CF₃, q, $J = 3.7$ Hz), 127.56, 130.72 (CH-C-CF₃, q, $J = 32.4$ Hz), 143.55, 147.54, 147.57, 151.16, 155.13, 161.25; ¹⁹F NMR (376.46 MHz, CDCl₃) δ (ppm): -62.50 (s); HRESIMS (m/z): [M + H]⁺ Calcd for C₂₀H₁₆ClF₃NO₃, 410.07653; found, 410.07736.

4.1.12. Synthesis of the target propoxy derivatives of 1,3-dioxoloarylquinolines (12a–d)

The target dioxolo derivatives **12a–d** have been synthesised utilising the synthetic procedures used for **6a–o** using imidazole or morpholine with the appropriate key intermediate **11a,b**.

4.1.12.1. 8-(3-(1H-imidazol-1-yl)propoxy)-6-(4-chlorophenyl)-[1,3]dioxolo[4,5-g]quinoline (12a). White solid, Yield 77%, m.p. 146–148 °C; ¹H NMR (400 MHz, CDCl₃) δ (ppm): 2.39 (p, 2H, CH₂, $J = 6.2$ Hz), 4.16 (t, 2H, CH₂-N, $J = 5.7$ Hz), 4.28 (t, 2H, CH₂-O, $J = 6.7$ Hz), 6.10 (s, 2H, dioxolo CH₂), 6.93 (s, 1H, imidazole CH), 6.94 (s, 1H, vinyl CH), 7.07 (s, 1H, imidazole CH), 7.38 (s, 1H, phenyl CH), 7.39 (s, 1H, phenyl CH), 7.43 (d, 2H, chlorophenyl 2CH, $J = 8.7$ Hz), 7.49 (s, 1H, imidazole CH), 7.95 (d, 2H, chlorophenyl 2CH, $J = 8.7$ Hz); ¹³C NMR (100 MHz, CDCl₃) δ (ppm): 30.54, 43.43, 64.18, 97.23, 97.46, 101.76, 106.13, 116.07, 118.90, 128.51, 128.85, 129.98, 135.12, 137.27, 138.49, 147.46, 147.53, 151.13, 155.48, 160.83; HRESIMS (m/z): [M + H]⁺ Calcd for C₂₂H₁₉ClN₃O₃, 408.11095; found, 408.11179; HPLC purity: 99.60%.

4.1.12.2. 6-(4-chlorophenyl)-8-(3-morpholinopropoxy)-[1,3]dioxolo[4,5-g]quinoline (12b). White solid, Yield 72%, m.p. 153–155 °C; ¹H NMR (400 MHz, CDCl₃) δ (ppm): 2.12 (p, 2H, CH₂, $J = 6.7$ Hz), 2.49 (t, 4H, morpholinyl 2CH₂, $J = 4.6$ Hz), 2.61 (t, 2H, CH₂-N, $J = 7.2$ Hz), 3.73 (t, 4H, morpholinyl 2CH₂, $J = 4.6$ Hz), 4.29 (t, 2H, CH₂-O, $J = 6.2$ Hz), 6.08 (s, 2H, dioxolo CH₂), 7.03 (s, 1H, vinyl CH), 7.36 (s, 1H, phenyl CH), 7.42 (s, 1H, phenyl CH), 7.44 (d, 2H, chlorophenyl 2CH, $J = 8.7$ Hz), 7.99 (d, 2H, chlorophenyl 2CH, $J = 8.7$ Hz); ¹³C NMR (100 MHz, CDCl₃) δ (ppm): 26.27, 53.82, 55.47, 66.43, 66.98, 97.50, 97.66, 101.63, 105.97, 116.35, 128.53, 128.82, 135.00, 138.76, 147.21, 147.44, 150.97, 155.51, 161.49; HRESIMS (m/z): [M + H]⁺ Calcd for C₂₃H₂₄ClN₂O₄, 427.14191; found, 427.14221; HPLC purity: 98.94%.

4.1.12.3. 8-(3-(1H-imidazol-1-yl)propoxy)-6-(4-(trifluoromethyl)phenyl)-[1,3]dioxolo[4,5-g]quinoline (12c). White solid, Yield 81%, m.p. 125–127 °C; ¹H NMR (400 MHz, CDCl₃) δ (ppm): 2.41 (p, 2H, CH₂, $J = 6.2$ Hz), 4.19 (t, 2H, CH₂-N, $J = 5.7$ Hz), 4.29 (t, 2H, CH₂-O, $J = 6.7$ Hz), 6.12 (s, 2H, dioxolo CH₂), 6.93 (s, 1H, imidazole CH), 7 (s, 1H, vinyl CH), 7.08 (s, 1H, imidazole CH), 7.41 (s, 2H, phenyl 2CH), 7.49 (s, 1H, imidazole CH), 7.72 (d, 2H, CF₃-phenyl 2CH, $J = 8.2$ Hz), 8.12 (d, 2H, CF₃-phenyl 2CH, $J = 8.2$ Hz); ¹³C NMR (100 MHz, CDCl₃) δ (ppm): 30.52, 43.42, 64.26, 97.22, 97.79, 101.83, 106.22, 16.34, 118.88, 124.22 (CF₃, q, $J = 272.7$ Hz), 125.61 (CH-C-CF₃, q, $J = 3.7$ Hz), 127.55, 130.01, 130.79 (CH-C-CF₃, q, $J = 33.2$ Hz), 137.28, 143.41, 147.60, 147.73, 151.26, 155.15, 160.92; ¹⁹F NMR (376.46 MHz, CDCl₃) δ (ppm): -62.52 (s); HRESIMS (m/z): [M + H]⁺ Calcd for C₂₃H₁₉F₃N₃O₃, 442.13730; found, 442.13754; HPLC purity: 99.35%.

4.1.12.4. 8-(3-morpholinopropoxy)-6-(4-(trifluoromethyl)phenyl)-[1,3]dioxolo[4,5-g]quinoline (12d). White solid, Yield 76%, m.p. 138–140 °C; ¹H NMR (400 MHz, CDCl₃) δ (ppm): 2.14 (p, 2H, CH₂,

$J = 6.7$ Hz), 2.50 (t, 4H, morpholinyl 2CH₂, $J = 4.4$ Hz), 2.62 (t, 2H, CH₂-N, $J = 7.2$ Hz), 3.73 (t, 4H, morpholinyl 2CH₂, $J = 4.4$ Hz), 4.32 (t, 2H, CH₂-O, $J = 6.2$ Hz), 6.10 (s, 2H, dioxolo CH₂), 7.08 (s, 1H, vinyl CH), 7.39 (s, 1H, phenyl CH), 7.44 (s, 1H, phenyl CH), 7.73 (d, 2H, CF₃-phenyl 2CH, $J = 8.2$ Hz), 8.16 (d, 2H, CF₃-phenyl 2CH, $J = 8.2$ Hz); ¹³C NMR (100 MHz, CDCl₃) δ (ppm): 26.27, 53.82, 55.45, 66.51, 66.98, 97.65, 97.83, 101.70, 106.05, 116.62, 124.23 (CF₃, q, $J = 272.3$ Hz), 125.59 (CH-C-CF₃, q, $J = 3.9$ Hz), 127.57, 130.70 (CH-C-CF₃, q, $J = 32.2$ Hz), 143.70, 147.48, 147.51, 151.10, 155.18, 161.59; ¹⁹F NMR (376.46 MHz, CDCl₃) δ (ppm): -62.50 (s); HRESIMS (m/z): [M + H]⁺ Calcd for C₂₄H₂₄F₃N₂O₄, 461.16827; found, 461.16837; HPLC purity: 99.62%.

4.1.13. Synthesis of 1-(2-amino-5-bromophenyl)ethan-1-one (13)

The 5-bromo derivative of 2-aminoacetophenone **13** has been synthesised based on the reported procedure^{46,47}.

Yellow solid, Yield 96%, m.p. 77–79 °C; ¹H NMR (400 MHz, CDCl₃) δ (ppm): 2.55 (s, 3H, CH₃), 6.29 (s, 2H, NH₂), 6.54 (d, 1H, phenyl CH, $J = 8.8$ Hz), 7.31 (dd, 1H, phenyl CH, $J = 2.3, 8.8$ Hz), 7.78 (d, 1H, phenyl CH, $J = 2.3$ Hz); ¹³C NMR (100 MHz, CDCl₃) δ (ppm): 27.83, 106.63, 118.99, 119.40, 134.11, 136.99, 149.08, 199.64; HRESIMS (m/z): [M + H]⁺ Calcd for C₈H₉ClBrNO, 213.98620; found, 213.98599.

4.1.14. Synthesis of 6-bromo-2-arylquinolones (14a,b)

1-(2-amino-5-bromophenyl)ethan-1-one **13** was benzoylated with *p*-chloro or fluorobenzoyl chloride using the same procedure for **3a–c**. Then, the resulted benzoyl derivatives have been subjected to ring closure reaction according to the synthetic route for **4a–c** to afford the corresponding 6-bromo-2-arylquinolones **14a,b**.

4.1.14.1. 6-bromo-2-(4-chlorophenyl)quinolin-4(1H)-one (14a).

Yellow solid, Yield 95%, m.p. > 250 °C; ¹H NMR (400 MHz, CDCl₃) δ (ppm): 6.41 (s, 1H, vinyl CH), 7.67 (d, 2H, chlorophenyl 2CH, $J = 8.5$ Hz), 7.72 (d, 1H, bromophenyl CH, $J = 8.9$ Hz), 7.84 (dd, 1H, bromophenyl CH, $J = 1.7, 8.9$ Hz), 7.87 (d, 2H, chlorophenyl 2CH, $J = 8.5$ Hz), 8.17 (d, 1H, bromophenyl CH, $J = 1.7$ Hz), 11.91 (s, 1H, NH); ¹³C NMR (100 MHz, CDCl₃) δ (ppm): 108.25, 116.52, 121.86, 126.76, 127.35, 129.53, 129.81, 133.14, 135.15, 135.96, 139.85, 149.64, 176.06; HRESIMS (m/z): [M + H]⁺ Calcd for C₁₅H₁₀BrClNO, 333.96288; found, 333.96295.

4.1.14.2. 6-bromo-2-(4-fluorophenyl)quinolin-4(1H)-one (14b).

Yellow solid, Yield 93%, m.p. > 250 °C; ¹H NMR (400 MHz, CDCl₃) δ (ppm): 6.39 (s, 1H, vinyl CH), 7.44 (t, 2H, fluorophenyl 2CH, $J = 8.7$ Hz), 7.72 (d, 1H, bromophenyl CH, $J = 8.8$ Hz), 7.84 (dd, 1H, bromophenyl CH, $J = 2.3, 8.8$ Hz), 7.91 (dd, 2H, fluorophenyl 2CH, $J = 5.4, 8.7$ Hz), 8.18 (d, 1H, bromophenyl CH, $J = 2.3$ Hz), 11.88 (s, 1H, NH); ¹³C NMR (100 MHz, CDCl₃) δ (ppm): 108.14, 116.44, 116.50 (CH-C-F, d, $J = 21.8$ Hz), 121.83, 126.72, 127.35, 130.43 (CH-C-F, d, $J = 8.7$ Hz), 130.85, 135.07, 139.85, 149.88, 163.95 (C-F, d, $J = 248.3$ Hz), 176.02; ¹⁹F NMR (376.46 MHz, CDCl₃) δ (ppm): -110.21 (s); HRESIMS (m/z): [M + H]⁺ Calcd for C₁₅H₁₀BrFNO, 317.99243; found, 317.99265.

4.1.15. Synthesis of 6-bromo-2-arylquinolones key intermediates (15a,b)

The key intermediates **15a,b** have been prepared from **14a,b** according to the synthetic route for **5a–c**.

4.1.15.1. 6-bromo-2-(4-chlorophenyl)-4-(3-chloropropoxy)quinoline (15a). White solid, Yield 96%, m.p. 134–136 °C; ^1H NMR (400 MHz, CDCl_3) δ (ppm): 2.44 (p, 2H, CH_2 , $J=6$ Hz), 3.86 (t, 2H, CH_2Cl , $J=6.1$ Hz), 4.43 (t, 2H, $\text{CH}_2\text{-O}$, $J=5.9$ Hz), 7.15 (s, 1H, vinyl CH), 7.47 (d, 2H, chlorophenyl 2CH, $J=8.6$ Hz), 7.76 (dd, 1H, bromophenyl CH, $J=2.2$, 9 Hz), 7.92 (d, 1H, bromophenyl CH, $J=9$ Hz), 8.04 (d, 2H, chlorophenyl 2CH, $J=8.6$ Hz), 8.26 (d, 1H, bromophenyl CH, $J=2.2$ Hz); ^{13}C NMR (100 MHz, CDCl_3) δ (ppm): 31.84, 41.23, 65.02, 98.77, 119.50, 121.47, 124.04, 128.76, 128.99, 131.03, 133.57, 135.78, 138.13, 147.77, 157.72, 160.98; HRESIMS (m/z): $[\text{M} + \text{H}]^+$ Calcd for $\text{C}_{18}\text{H}_{15}\text{BrCl}_2\text{NO}$, 409.97088; found, 409.97205.

4.1.15.2. 6-bromo-4-(3-chloropropoxy)-2-(4-fluorophenyl)quinoline (15b). White solid, Yield 92%, m.p. 163–165 °C; ^1H NMR (400 MHz, CDCl_3) δ (ppm): 2.44 (p, 2H, CH_2 , $J=6$ Hz), 3.86 (t, 2H, CH_2Cl , $J=6.1$ Hz), 4.43 (t, 2H, $\text{CH}_2\text{-O}$, $J=5.9$ Hz), 7.15 (s, 1H, vinyl CH), 7.19 (t, 2H, fluorophenyl 2CH, $J=8.8$ Hz), 7.75 (dd, 1H, bromophenyl CH, $J=2.3$, 9 Hz), 7.93 (d, 1H, bromophenyl CH, $J=9$ Hz), 8.09 (dd, 2H, fluorophenyl 2CH, $J=5.4$, 8.8 Hz), 8.27 (d, 1H, bromophenyl CH, $J=2.3$ Hz); ^{13}C NMR (100 MHz, CDCl_3) δ (ppm): 31.85, 41.22, 65.00, 98.84, 115.77 (CH-C-F, d, $J=21.7$ Hz), 119.33, 121.37, 124.03, 129.38 (CH-CH-C-F, d, $J=8.6$ Hz), 130.98, 133.52, 135.91 (C-CH-CH-C-F, d, $J=3$ Hz), 147.78, 157.97, 160.94, 163.89 (C-F, d, $J=249.4$ Hz); ^{19}F NMR (376.46 MHz, CDCl_3) δ (ppm): -111.96 (s); HRESIMS (m/z): $[\text{M} + \text{H}]^+$ Calcd for $\text{C}_{18}\text{H}_{15}\text{BrClFNO}$, 394.00041; found, 394.00122.

4.1.16. Synthesis of the target 6-bromo-4-propoxy-2-arylquinolines (16a–d)

The synthesis of the target 6-bromo-4-propoxy-2-arylquinolines **16a–d** has been accomplished based on the general synthetic route for **6a–o** utilising imidazole or morpholine with the respective key intermediate **15a,b**.

4.1.16.1. 4-(3-(1H-imidazol-1-yl)propoxy)-6-bromo-2-(4-chlorophenyl)quinoline (16a). White solid, Yield 84%, m.p. 149–151 °C; ^1H NMR (400 MHz, CDCl_3) δ (ppm): 2.44 (p, 2H, CH_2 , $J=6.2$ Hz), 4.19 (t, 2H, $\text{CH}_2\text{-N}$, $J=5.7$ Hz), 4.31 (t, 2H, $\text{CH}_2\text{-O}$, $J=6.6$ Hz), 6.95 (s, 1H, imidazole CH), 7.04 (s, 1H, vinyl CH), 7.09 (s, 1H, imidazole CH), 7.46 (d, 2H, chlorophenyl 2CH, $J=8.7$ Hz), 7.50 (s, 1H, imidazole CH), 7.78 (dd, 1H, bromophenyl CH, $J=2.2$, 9 Hz), 7.94 (d, 1H, bromophenyl CH, $J=9$ Hz), 8 (d, 2H, chlorophenyl 2CH, $J=8.7$ Hz), 8.27 (d, 1H, bromophenyl CH, $J=2.2$ Hz); ^{13}C NMR (100 MHz, CDCl_3) δ (ppm): 30.42, 43.41, 64.59, 98.77, 118.87, 119.69, 121.33, 123.79, 128.75, 129.00, 130.09, 131.15, 133.71, 135.86, 137.28, 137.99, 147.81, 157.74, 160.67; HRESIMS (m/z): $[\text{M} + \text{H}]^+$ Calcd for $\text{C}_{21}\text{H}_{18}\text{BrClN}_3\text{O}$, 442.03163; found, 442.03214; HPLC purity: 98.60%.

4.1.16.2. 4-(3-((6-bromo-2-(4-chlorophenyl)quinolin-4-yl)oxy)propyl)morpholine (16b). White solid, Yield 78%, m.p. 137–139 °C; ^1H NMR (400 MHz, CDCl_3) δ (ppm): 2.15 (p, 2H, CH_2 , $J=6.7$ Hz), 2.50 (t, 4H, morpholinyl 2 CH_2 , $J=4.4$ Hz), 2.62 (t, 2H, $\text{CH}_2\text{-N}$, $J=7.1$ Hz), 3.73 (t, 4H, morpholinyl 2 CH_2 , $J=4.4$ Hz), 4.33 (t, 2H, $\text{CH}_2\text{-O}$, $J=6.3$ Hz), 7.13 (s, 1H, vinyl CH), 7.47 (d, 2H, chlorophenyl 2CH, $J=8.6$ Hz), 7.75 (dd, 1H, bromophenyl CH, $J=2.2$, 9 Hz), 7.92 (d, 1H, bromophenyl CH, $J=9$ Hz), 8.03 (d, 2H, chlorophenyl 2CH, $J=8.6$ Hz), 8.30 (d, 1H, bromophenyl CH, $J=2.2$ Hz); ^{13}C NMR (100 MHz, CDCl_3) δ (ppm): 26.14, 53.81, 55.37, 66.84, 66.98, 98.76, 119.38, 121.63, 124.21, 128.77, 128.97, 130.96, 133.49, 135.71, 138.28, 147.76, 157.75, 161.34; HRESIMS (m/z): $[\text{M} + \text{H}]^+$ Calcd for

$\text{C}_{22}\text{H}_{23}\text{BrClN}_2\text{O}_2$, 461.06259; found, 461.06314; HPLC purity: 99.92%.

4.1.16.3. 4-(3-(1H-imidazol-1-yl)propoxy)-6-bromo-2-(4-fluorophenyl)quinoline (16c). White solid, Yield 80%, m.p. 144–146 °C; ^1H NMR (400 MHz, CDCl_3) δ (ppm): 2.43 (p, 2H, CH_2 , $J=6.2$ Hz), 4.19 (t, 2H, $\text{CH}_2\text{-N}$, $J=5.7$ Hz), 4.31 (t, 2H, $\text{CH}_2\text{-O}$, $J=6.6$ Hz), 6.94 (s, 1H, imidazole CH), 7.03 (s, 1H, vinyl CH), 7.09 (s, 1H, imidazole CH), 7.17 (t, 2H, fluorophenyl 2CH, $J=8.7$ Hz), 7.50 (s, 1H, imidazole CH), 7.77 (dd, 1H, bromophenyl CH, $J=2.3$, 9 Hz), 7.94 (d, 1H, bromophenyl CH, $J=9$ Hz), 8.04 (dd, 2H, fluorophenyl 2CH, $J=5.4$, 8.7 Hz), 8.27 (d, 1H, bromophenyl CH, $J=2.3$ Hz); ^{13}C NMR (100 MHz, CDCl_3) δ (ppm): 30.42, 43.41, 64.55, 98.83, 115.78 (CH-C-F, d, $J=21.6$ Hz), 118.88, 119.51, 121.22, 123.78, 129.37 (CH-CH-C-F, d, $J=8.5$ Hz), 130.07, 131.10, 133.65, 135.75 (C-CH-CH-C-F, d, $J=3.1$ Hz), 137.28, 147.80, 157.97, 160.61, 163.91 (C-F, d, $J=249.5$ Hz); ^{19}F NMR (376.46 MHz, CDCl_3) δ (ppm): -111.81 (s); HRESIMS (m/z): $[\text{M} + \text{H}]^+$ Calcd for $\text{C}_{21}\text{H}_{18}\text{BrFN}_3\text{O}$, 426.06118; found, 426.06125; HPLC purity: 99.65%.

4.1.16.4. 4-(3-((6-bromo-2-(4-fluorophenyl)quinolin-4-yl)oxy)propyl)morpholine (16d). White solid, Yield 87%, m.p. 132–134 °C; ^1H NMR (400 MHz, CDCl_3) δ (ppm): 2.16 (p, 2H, CH_2 , $J=6.7$ Hz), 2.51 (t, 4H, morpholinyl 2 CH_2 , $J=4.4$ Hz), 2.62 (t, 2H, $\text{CH}_2\text{-N}$, $J=7.1$ Hz), 3.73 (t, 4H, morpholinyl 2 CH_2 , $J=4.4$ Hz), 4.33 (t, 2H, $\text{CH}_2\text{-O}$, $J=6.2$ Hz), 7.12 (s, 1H, vinyl CH), 7.19 (t, 2H, fluorophenyl 2CH, $J=8.7$ Hz), 7.75 (dd, 1H, bromophenyl CH, $J=2.3$, 9 Hz), 7.92 (d, 1H, bromophenyl CH, $J=9$ Hz), 8.08 (dd, 2H, fluorophenyl 2CH, $J=5.4$, 8.7 Hz), 8.17 (d, 1H, bromophenyl CH, $J=2.3$ Hz); ^{13}C NMR (100 MHz, CDCl_3) δ (ppm): 26.14, 53.81, 55.37, 66.81, 66.97, 98.83, 115.74 (CH-C-F, d, $J=21.7$ Hz), 119.21, 121.52, 124.19, 129.37 (CH-CH-C-F, d, $J=8.5$ Hz), 130.91, 133.44, 136.05 (C-CH-CH-C-F, d, $J=2.6$ Hz), 147.76, 158.01, 161.28, 163.85 (C-F, d, $J=249.4$ Hz); ^{19}F NMR (376.46 MHz, CDCl_3) δ (ppm): -112.05 (s); HRESIMS (m/z): $[\text{M} + \text{H}]^+$ Calcd for $\text{C}_{22}\text{H}_{23}\text{BrFN}_2\text{O}_2$, 445.09215; found, 445.09241; HPLC purity: 99.15%.

4.1.17. Synthesis of 5-aryl-2-aminoacetophenones (17a,b)

To a mixture of 1-(2-amino-5-bromophenyl)ethan-1-one **13** (1.07 g, 5 mmol), 4-methoxyphenylboronic acid or 2-furylboronic acid (5.5 mmol), K_2CO_3 (2.28 g, 16.5 mmol) and $\text{Pd}(\text{PPh}_3)_4$ (0.02 equivalent, 116 mg), dioxane (14 ml) and H_2O (14 ml) were added under N_2 atmosphere. The reaction mixture was refluxed under N_2 at 100 °C for 4 h. Then, the reaction mixture was poured into ethylacetate (50 ml) and the organic layer was separated. The aqueous layer was extracted with ethylacetate (30 \times 3) and the organic layers were collected and washed with 1 M HCl (100 \times 3) then brine ((100 \times 3). After evaporation of the organic solvent under vacuum, the residue was purified by silica gel column chromatography using hexane/ethylacetate to afford the corresponding compounds **17a,b**.

4.1.17.1. 1-(4-amino-4'-methoxy-[1,1'-biphenyl]-3-yl)ethan-1-one (17a). Yellow solid, Yield 86%, m.p. 101–103 °C; ^1H NMR (400 MHz, CDCl_3) δ (ppm): 2.63 (s, 3H, $\text{CH}_3\text{-C=O}$), 3.85 (s, 3H, $\text{CH}_3\text{-O}$), 6.29 (s, 2H, NH_2), 6.71 (d, 1H, phenyl CH, $J=8.6$ Hz), 6.97 (d, 2H, methoxyphenyl 2CH, $J=8.8$ Hz), 7.45 (d, 2H, methoxyphenyl 2CH, $J=8.8$ Hz), 7.48 (dd, 1H, phenyl CH, $J=2.2$, 8.6 Hz), 7.76 (d, 1H, phenyl CH, $J=2.2$ Hz); ^{13}C NMR (100 MHz, CDCl_3) δ (ppm): 27.93, 55.39, 114.29, 117.73, 118.44, 127.36, 128.80, 129.83, 133.08,

133.24, 149.15, 158.66, 200.79; HRESIMS (m/z): $[M + H]^+$ Calcd for $C_{15}H_{16}NO_2$, 242.11756; found, 242.11717.

4.1.17.2. 1-(2-amino-5-(furan-2-yl)phenyl)ethan-1-one (17b). Yellow solid, Yield 70%, m.p. 87–89 °C; 1H NMR (400 MHz, $CDCl_3$) δ (ppm): 2.63 (s, 3H, CH_3), 6.36 (s, 2H, NH_2), 6.44–6.46 (m, 2H, furyl 2CH), 6.66 (d, 1H, phenyl CH, $J=8.6$ Hz), 7.41 (dd, 1H, furyl CH, $J=0.9, 1.6$ Hz), 7.55 (dd, 1H, phenyl CH, $J=2, 8.6$ Hz), 8.02 (d, 1H, phenyl CH, $J=2$ Hz); ^{13}C NMR (100 MHz, $CDCl_3$) δ (ppm): 27.91, 102.61, 111.55, 117.61, 118.02, 119.47, 127.24, 130.41, 141.09, 149.57, 153.73, 200.74; HRESIMS (m/z): $[M + H]^+$ Calcd for $C_{12}H_{12}NO_2$, 202.08626; found, 202.08594.

4.1.18. Synthesis of 2,6-diarylquinolones (18a–c)

The synthesis of 2,6-diarylquinolones **18a–c** has been accomplished using 5-aryl-2-aminoacetophenones **17a,b** and the respective *p*-chloro or fluorobenzoyl chloride according to the synthetic route used for 6-bromo-2-arylquinolones **14a,b**. The 2,6-diarylquinolones **18a,b** have poor solubility for NMR spectral analysis, so the NMR spectral analysis of the soluble 6-furyl analog **18c** was used for their structural authentication in addition to HRMS for **18a,b**. Moreover, the corresponding 4-propoxy analogs **19a–c** exhibited good solubility and their spectral characterisation was enough for structural confirmation of 2,6-diarylquinolones **18a–c**.

4.1.18.1. 2-(4-chlorophenyl)-6-(4-methoxyphenyl)quinolin-4(1H)-one (18a). Yellow solid, Yield 97%, m.p. > 250 °C; HRESIMS (m/z): $[M + Na]^+$ Calcd for $C_{22}H_{16}ClNO_2Na$, 384.07618; found, 384.07623.

4.1.18.2. 2-(4-fluorophenyl)-6-(4-methoxyphenyl)quinolin-4(1H)-one (18b). Yellow solid, Yield 90%, m.p. > 250 °C; HRESIMS (m/z): $[M + H]^+$ Calcd for $C_{22}H_{16}FNO_2Na$, 368.10573; found, 368.10574.

4.1.18.3. 2-(4-chlorophenyl)-6-(furan-2-yl)quinolin-4(1H)-one (18c). Yellow solid, Yield 93%, m.p. > 250 °C; 1H NMR (400 MHz, $CDCl_3$) δ (ppm): 6.68 (dd, 1H, furyl CH, $J=1.6, 3.4$ Hz), 7.04 (s, 1H, vinyl CH), 7.19 (d, 1H, furyl CH, $J=3.4$ Hz), 7.73 (d, 2H, chlorophenyl 2CH, $J=8.6$ Hz), 7.86 (d, 1H, furyl CH, $J=1.6$ Hz), 7.99 (d, 2H, chlorophenyl 2CH, $J=8.6$ Hz), 8.18 (d, 1H, phenyl CH, $J=8.9$ Hz), 8.26 (dd, 1H, phenyl CH, $J=2, 8.9$ Hz), 8.43 (d, 1H, phenyl CH, $J=2$ Hz); ^{13}C NMR (100 MHz, $CDCl_3$) δ (ppm): 106.42, 108.09, 112.95, 117.53, 121.27, 122.67, 128.11, 129.59, 129.71, 130.49, 132.12, 136.85, 140.05, 144.39, 151.67, 152.32, 172.86; HRESIMS (m/z): $[M + H]^+$ Calcd for $C_{19}H_{13}ClNO_2$, 322.06293; found, 322.06299.

4.1.19. Synthesis of 4-propoxy-2,6-diarylquinolines key intermediates (19a–c)

The key intermediates 4-propoxy-2,6-diarylquinolines **19a–c** were synthesised from 2,6-diarylquinolones **18a–c** utilising the synthetic route used for **5a–c**.

4.1.19.1. 2-(4-chlorophenyl)-4-(3-chloropropoxy)-6-(4-methoxyphenyl)quinoline (19a). Off-white solid, Yield 93%, m.p. 183–185 °C; 1H NMR (400 MHz, $CDCl_3$) δ (ppm): 2.45 (p, 2H, CH_2 , $J=6.2$ Hz), 3.86 (t, 2H, CH_2Cl , $J=6.2$ Hz), 3.88 (s, 3H, CH_3-O), 4.45 (t, 2H, CH_2-O , $J=5.8$ Hz), 7.04 (d, 2H, methoxyphenyl 2CH, $J=8.8$ Hz), 7.15 (s, 1H, vinyl CH), 7.48 (d, 2H, chlorophenyl 2CH, $J=8.6$ Hz), 7.66 (d, 2H, methoxyphenyl 2CH, $J=8.8$ Hz), 7.94 (dd, 1H, phenyl CH, $J=2, 8.8$ Hz), 8.07 (d, 2H, chlorophenyl 2CH, $J=8.6$ Hz), 8.11 (d, 1H, phenyl CH, $J=8.8$ Hz), 8.26 (d, 1H, phenyl CH, $J=2$ Hz); ^{13}C NMR

(100 MHz, $CDCl_3$) δ (ppm): 31.95, 41.34, 55.41, 64.90, 98.43, 114.41, 118.46, 120.52, 128.48, 128.76, 128.93, 129.59, 129.68, 133.16, 135.43, 138.06, 138.60, 148.31, 156.99, 159.47, 161.94; HRESIMS (m/z): $[M + H]^+$ Calcd for $C_{25}H_{22}Cl_2NO_2$, 438.10221; found, 438.10242.

4.1.19.2. 4-(3-chloropropoxy)-2-(4-fluorophenyl)-6-(4-methoxyphenyl)quinoline (19b). Off-white solid, Yield 86%, m.p. 174–176 °C; 1H NMR (400 MHz, $CDCl_3$) δ (ppm): 2.46 (p, 2H, CH_2 , $J=6.2$ Hz), 3.86 (t, 2H, CH_2Cl , $J=6.2$ Hz), 3.88 (s, 3H, CH_3-O), 4.46 (t, 2H, CH_2-O , $J=5.8$ Hz), 7.04 (d, 2H, methoxyphenyl 2CH, $J=8.8$ Hz), 7.16 (s, 1H, vinyl CH), 7.20 (t, 2H, fluorophenyl 2CH, $J=8.7$ Hz), 7.66 (d, 2H, methoxyphenyl 2CH, $J=8.8$ Hz), 7.93 (dd, 1H, phenyl CH, $J=2, 8.8$ Hz), 8.09–8.13 (m, 3H, fluorophenyl 2CH, phenyl CH), 8.27 (d, 1H, phenyl CH, $J=2$ Hz); ^{13}C NMR (100 MHz, $CDCl_3$) δ (ppm): 31.96, 41.35, 55.41, 64.88, 98.51, 114.41, 115.68 ($\underline{CH-C-F}$, d, $J=21.7$ Hz), 118.47, 120.40, 128.48, 129.34 ($\underline{CH-CH-C-F}$, d, $J=8.5$ Hz), 129.55, 129.63, 133.22, 136.38 ($\underline{C-CH-CH-C-F}$, d, $J=3$ Hz), 137.94, 148.32, 157.26, 159.44, 161.90, 163.75 (C-F, d, $J=248.8$ Hz); ^{19}F NMR (376.46 MHz, $CDCl_3$) δ (ppm): –112.55 (s); HRESIMS (m/z): $[M + H]^+$ Calcd for $C_{25}H_{22}ClFNO_2$, 422.13176; found, 422.13123.

4.1.19.3. 2-(4-chlorophenyl)-4-(3-chloropropoxy)-6-(furan-2-yl)quinoline (19c). Yellow solid, Yield 74%, m.p. 144–146 °C; 1H NMR (400 MHz, $CDCl_3$) δ (ppm): 2.47 (p, 2H, CH_2 , $J=6.2$ Hz), 3.88 (t, 2H, CH_2Cl , $J=6.2$ Hz), 4.44 (t, 2H, CH_2-O , $J=5.8$ Hz), 6.53 (dd, 1H, furyl CH, $J=1.7, 3.4$ Hz), 6.79 (d, 1H, furyl CH, $J=3.4$ Hz), 7.14 (s, 1H, vinyl CH), 7.47 (d, 2H, chlorophenyl 2CH, $J=8.6$ Hz), 7.55 (d, 1H, furyl CH, $J=1.7$ Hz), 7.98 (dd, 1H, phenyl CH, $J=1.9, 8.8$ Hz), 8.06 (d, 3H, chlorophenyl 2CH, phenyl CH, $J=8.6$ Hz), 8.38 (d, 1H, phenyl CH, $J=1.9$ Hz); ^{13}C NMR (100 MHz, $CDCl_3$) δ (ppm): 31.94, 41.36, 64.95, 98.60, 106.15, 111.95, 115.65, 120.52, 126.56, 128.02, 128.72, 128.93, 129.71, 135.50, 138.43, 142.63, 148.55, 153.66, 157.06, 161.94; HRESIMS (m/z): $[M + H]^+$ Calcd for $C_{22}H_{18}Cl_2NO_2$, 398.07091; found, 398.07150.

4.1.20. Synthesis of the target 4-propoxy-2,6-diarylquinolines (20a–f)

The synthesis of the target 4-propoxy-2,6-diarylquinolines **20a–f** has been conducted by reaction of imidazole or morpholine with the corresponding key intermediate **19a–c** under the same conditions used for synthesis of **6a–o**.

4.1.20.1. 4-(3-(1H-imidazol-1-yl)propoxy)-2-(4-chlorophenyl)-6-(4-methoxyphenyl)quinoline (20a). White solid, Yield 80%, m.p. 210–212 °C; 1H NMR (400 MHz, $CDCl_3$) δ (ppm): 2.45 (p, 2H, CH_2 , $J=6.2$ Hz), 3.88 (s, 3H, CH_3-O), 4.22 (t, 2H, CH_2-N , $J=5.7$ Hz), 4.31 (t, 2H, CH_2-O , $J=6.6$ Hz), 6.94 (s, 1H, imidazole CH), 7.04 (d, 2H, methoxyphenyl 2CH, $J=8.8$ Hz), 7.05 (s, 1H, vinyl CH), 7.08 (s, 1H, imidazole CH), 7.47 (d, 2H, chlorophenyl 2CH, $J=8.6$ Hz), 7.50 (s, 1H, imidazole CH), 7.67 (d, 2H, methoxyphenyl 2CH, $J=8.8$ Hz), 7.95 (dd, 1H, phenyl CH, $J=2, 8.8$ Hz), 8.03 (d, 2H, chlorophenyl 2CH, $J=8.6$ Hz), 8.13 (d, 1H, phenyl CH, $J=8.8$ Hz), 8.27 (d, 1H, phenyl CH, $J=2$ Hz); ^{13}C NMR (100 MHz, $CDCl_3$) δ (ppm): 30.50, 43.45, 55.43, 64.38, 98.41, 114.47, 118.18, 118.90, 120.40, 128.50, 128.74, 128.94, 129.74, 129.83, 130.05, 133.11, 135.51, 137.30, 138.30, 138.45, 148.35, 156.97, 159.54, 161.61; HRESIMS (m/z): $[M + H]^+$ Calcd for $C_{28}H_{25}ClN_3O_2$, 470.16298; found, 470.16299; HPLC purity: 99.88%.

4.1.20.2. 4-(3-((2-(4-chlorophenyl)-6-(4-methoxyphenyl)quinolin-4-yl)oxy)propyl)morpholine (20b). White solid, Yield 89%, m.p. 173–175 °C; ^1H NMR (400 MHz, CDCl_3) δ (ppm): 2.18 (p, 2H, CH_2 , $J=6.7$ Hz), 2.50 (t, 4H, morpholinyl 2CH_2 , $J=4.4$ Hz), 2.63 (t, 2H, $\text{CH}_2\text{-N}$, $J=7.1$ Hz), 3.73 (t, 4H, morpholinyl 2CH_2 , $J=4.4$ Hz), 3.88 (s, 3H, $\text{CH}_3\text{-O}$), 4.35 (t, 2H, $\text{CH}_2\text{-O}$, $J=6.3$ Hz), 7.03 (d, 2H, methoxyphenyl 2CH, $J=8.8$ Hz), 7.13 (s, 1H, vinyl CH), 7.48 (d, 2H, chlorophenyl 2CH, $J=8.6$ Hz), 7.67 (d, 2H, methoxyphenyl 2CH, $J=8.8$ Hz), 7.93 (dd, 1H, phenyl CH, $J=2.1$, 8.8 Hz), 8.06 (d, 2H, chlorophenyl 2CH, $J=8.6$ Hz), 8.10 (d, 1H, phenyl CH, $J=8.8$ Hz), 8.30 (d, 1H, phenyl CH, $J=2.1$ Hz); ^{13}C NMR (100 MHz, CDCl_3) δ (ppm): 26.22, 53.83, 55.41, 55.48, 66.64, 66.98, 98.40, 114.40, 118.59, 120.66, 128.44, 128.77, 128.90, 129.48, 129.63, 133.20, 135.37, 137.91, 138.74, 148.30, 157.02, 159.44, 162.28; HRESIMS (m/z): $[\text{M} + \text{H}]^+$ Calcd for $\text{C}_{29}\text{H}_{30}\text{ClN}_2\text{O}_3$, 489.19395; found, 489.19415; HPLC purity: 96.78%.

4.1.20.3. 4-(3-(1H-imidazol-1-yl)propoxy)-2-(4-fluorophenyl)-6-(4-methoxyphenyl)quinoline (20c). White solid, Yield 79%, m.p. 176–178 °C; ^1H NMR (400 MHz, CDCl_3) δ (ppm): 2.44 (p, 2H, CH_2 , $J=6.2$ Hz), 3.88 (s, 3H, $\text{CH}_3\text{-O}$), 4.22 (t, 2H, $\text{CH}_2\text{-N}$, $J=5.7$ Hz), 4.30 (t, 2H, $\text{CH}_2\text{-O}$, $J=6.6$ Hz), 6.94 (s, 1H, imidazole CH), 7.04 (s, 1H, vinyl CH), 7.06 (d, 2H, methoxyphenyl 2CH, $J=8.8$ Hz), 7.07 (s, 1H, imidazole CH), 7.18 (t, 2H, fluorophenyl 2CH, $J=8.8$ Hz), 7.50 (s, 1H, imidazole CH), 7.67 (d, 2H, methoxyphenyl 2CH, $J=8.8$ Hz), 7.95 (dd, 1H, phenyl CH, $J=2$, 8.8 Hz), 8.07 (dd, 2H, fluorophenyl 2CH, $J=5.4$, 8.8 Hz), 8.13 (d, 1H, phenyl CH, $J=8.8$ Hz), 8.27 (d, 1H, phenyl CH, $J=2$ Hz); ^{13}C NMR (100 MHz, CDCl_3) δ (ppm): 30.51, 43.46, 55.42, 64.36, 98.48, 114.46, 115.69 (CH-C-F, d, $J=21.7$ Hz), 118.19, 118.91, 120.27, 128.49, 129.33 (CH-CH-C-F, d, $J=8.3$ Hz), 129.70, 129.77, 130.02, 133.15, 136.22, (C-CH-CH-C-F, d, $J=3.3$ Hz), 137.29, 138.16, 148.34, 157.23, 159.52, 161.57, 163.77 (C-F, d, $J=249.2$ Hz); ^{19}F NMR (376.46 MHz, CDCl_3) δ (ppm): -112.39 (s); HRESIMS (m/z): $[\text{M} + \text{H}]^+$ Calcd for $\text{C}_{28}\text{H}_{25}\text{FN}_3\text{O}_2$, 454.19326; found, 454.19244; HPLC purity: 99.21%.

4.1.20.4. 4-(3-((2-(4-fluorophenyl)-6-(4-methoxyphenyl)quinolin-4-yl)oxy)propyl)morpholine (20d). White solid, Yield 82%, m.p. 168–170 °C; ^1H NMR (400 MHz, CDCl_3) δ (ppm): 2.18 (p, 2H, CH_2 , $J=6.7$ Hz), 2.50 (t, 4H, morpholinyl 2CH_2 , $J=4.4$ Hz), 2.63 (t, 2H, $\text{CH}_2\text{-N}$, $J=7.1$ Hz), 3.73 (t, 4H, morpholinyl 2CH_2 , $J=4.4$ Hz), 3.88 (s, 3H, $\text{CH}_3\text{-O}$), 4.36 (t, 2H, $\text{CH}_2\text{-O}$, $J=6.3$ Hz), 7.03 (d, 2H, methoxyphenyl 2CH, $J=8.8$ Hz), 7.13 (s, 1H, vinyl CH), 7.20 (t, 2H, fluorophenyl 2CH, $J=8.7$ Hz), 7.67 (d, 2H, methoxyphenyl 2CH, $J=8.8$ Hz), 7.93 (dd, 1H, phenyl CH, $J=2$, 8.8 Hz), 8.09–8.12 (m, 3H, fluorophenyl 2CH, phenyl CH), 8.30 (d, 1H, phenyl CH, $J=2$ Hz); ^{13}C NMR (100 MHz, CDCl_3) δ (ppm): 26.23, 53.83, 55.40, 55.48, 66.62, 66.98, 98.48, 114.40, 115.65 (CH-C-F, d, $J=21.5$ Hz), 118.59, 120.54, 128.43, 129.34, (CH-CH-C-F, d, $J=8.5$ Hz), 129.44, 129.57, 133.25, 136.51 (C-CH-CH-C-F, d, $J=3$ Hz), 137.79, 148.30, 157.29, 159.42, 162.24, 163.71 (C-F, d, $J=248.8$ Hz); ^{19}F NMR (376.46 MHz, CDCl_3) δ (ppm): -112.63 (s); HRESIMS (m/z): $[\text{M} + \text{H}]^+$ Calcd for $\text{C}_{29}\text{H}_{30}\text{FN}_2\text{O}_3$, 473.22422; found, 473.22357; HPLC purity: 99.75%.

4.1.20.5. 4-(3-(1H-imidazol-1-yl)propoxy)-2-(4-chlorophenyl)-6-(furan-2-yl)quinoline (20e). Yellow solid, Yield 79%, m.p. 130–132 °C; ^1H NMR (400 MHz, CDCl_3) δ (ppm): 2.47 (p, 2H, CH_2 , $J=6.2$ Hz), 4.22 (t, 2H, $\text{CH}_2\text{-N}$, $J=5.7$ Hz), 4.34 (t, 2H, $\text{CH}_2\text{-O}$, $J=6.6$ Hz), 6.55 (dd, 1H, furyl CH, $J=1.6$, 3.3 Hz), 6.82 (d, 1H, furyl CH, $J=3.3$ Hz), 6.96 (s, 1H, imidazole CH), 7.04 (s, 1H, vinyl CH), 7.09 (s, 1H, imidazole CH), 7.46 (d, 2H, chlorophenyl 2CH,

$J=8.5$ Hz), 7.53 (s, 1H, imidazole CH), 7.56 (d, 1H, furyl CH, $J=1.6$ Hz), 7.99 (dd, 1H, phenyl CH, $J=1.8$, 8.7 Hz), 8.02 (d, 2H, chlorophenyl 2CH, $J=8.5$ Hz), 8.07 (d, 1H, phenyl CH, $J=8.7$ Hz), 8.41 (d, 1H, phenyl CH, $J=1.8$ Hz); ^{13}C NMR (100 MHz, CDCl_3) δ (ppm): 30.48, 43.47, 64.40, 98.63, 106.32, 112.03, 115.33, 118.94, 120.41, 126.70, 128.19, 128.71, 128.95, 129.87, 129.96, 135.58, 137.29, 138.30, 142.72, 148.59, 153.57, 157.09, 161.62; HRESIMS (m/z): $[\text{M} + \text{H}]^+$ Calcd for $\text{C}_{25}\text{H}_{21}\text{ClN}_3\text{O}_2$, 430.13168; found, 430.13174; HPLC purity: 95.27%.

4.1.20.6. 4-(3-((2-(4-chlorophenyl)-6-(furan-2-yl)quinolin-4-yl)oxy)propyl)morpholine (20f). Yellow solid, Yield 74%, m.p. 136–138 °C; ^1H NMR (400 MHz, CDCl_3) δ (ppm): 2.19 (p, 2H, CH_2 , $J=6.7$ Hz), 2.52 (t, 4H, morpholinyl 2CH_2 , $J=4.4$ Hz), 2.65 (t, 2H, $\text{CH}_2\text{-N}$, $J=7.1$ Hz), 3.74 (t, 4H, morpholinyl 2CH_2 , $J=4.4$ Hz), 4.35 (t, 2H, $\text{CH}_2\text{-O}$, $J=6.3$ Hz), 6.53 (dd, 1H, furyl CH, $J=1.8$, 3.4 Hz), 6.79 (dd, 1H, furyl CH, $J=0.5$, 3.4 Hz), 7.12 (s, 1H, vinyl CH), 7.47 (d, 2H, chlorophenyl 2CH, $J=8.6$ Hz), 7.54 (dd, 1H, furyl CH, $J=0.5$, 1.8 Hz), 7.98 (dd, 1H, phenyl CH, $J=1.9$, 8.8 Hz), 8.05 (d, 3H, chlorophenyl 2CH, phenyl CH, $J=8.6$ Hz), 8.42 (d, 1H, phenyl CH, $J=1.9$ Hz); ^{13}C NMR (100 MHz, CDCl_3) δ (ppm): 26.19, 53.84, 55.49, 66.71, 67.00, 98.60, 106.04, 111.94, 115.86, 120.67, 126.49, 127.93, 128.73, 128.91, 129.67, 135.44, 138.60, 142.58, 148.56, 153.75, 157.12, 162.29; HRESIMS (m/z): $[\text{M} + \text{H}]^+$ Calcd for $\text{C}_{26}\text{H}_{26}\text{ClN}_2\text{O}_3$, 449.16265; found, 449.16275; HPLC purity: 98.79%.

4.2. In vitro anticancer activity

4.2.1. In vitro antiproliferative assay

The antiproliferative assay against five cancer cell lines representing three different tumour subpanels, including colorectal (DLD-1, HCT-116), breast (MDMBA-231, MCF-7), and cervical (HeLa) cell lines was conducted using MTT assay. Cells were seeded at 1×10^4 cells/well and cultured overnight in a 96-well plate. The cells were treated with either 10 μM of tested quinolines **6a–o**, **8a,b**, **10a,b**, **12a–d**, **16a–d**, and **20a–f**, or DMSO as a negative control. After 24 h, the cells washed with phosphate buffered saline (PBS, Invitrogen Gibco) and incubated with 20 μl of MTT solution (2 mg/ml) for 4 h at 37 °C. Then, 150 μl DMSO was used to solubilise MTT formazan crystals. Finally, the plates were shaken, and the optical density was determined at 570 nm using ELISA plate reader. At least, three independent experiments were performed. Percentage of growth inhibition was determined as $(1 - [\text{OD of treated cells}/\text{OD of control cells}])$. On the other hand, using the MTT assay, we tested the effect of different concentrations (0.5, 1, 10, 30, 50, and 100 μM) of the synthesised compounds on colorectal cancer cell lines (DLD-1 and HCT-116), using DMSO as a negative control, whereas Gefitinib and TAE226 were used as positive controls. The IC_{50} values were calculated using Prism v0.8 software (GraphPad Software Inc., La Jolla, CA).

4.2.2. Apoptosis assay

The apoptotic effect of the most potent antiproliferative agents **6f**, **6h**, **6i**, **16d**, and **20f** on DLD-1 colorectal cancer cell line was investigated using the annexin V/propidium iodide (AV/PI) staining kit (BioLegend, San Diego, CA, USA) according to the manufacturer's instructions. DLD-1 cells were treated with 3 μM of the most potent antiproliferative compounds **6f**, **6h**, **6i**, **16d**, and **20f** or DMSO as a negative control then incubated for 24 h. Flow cytometric analysis was conducted using FACS Calibur flow cytometer (BD Biosciences, San Jose, CA, USA).

4.3. Topoisomerase I-mediated DNA cleavage assay

A 3'-[³²P]-labeled 117-bp DNA substrate oligonucleotide was prepared as described previously³⁹. Radiolabeled DNA was incubated with recombinant human TOP1 in 20 µL reaction buffer (10 mmol/L Tris-HCl, pH 7.5, 50 mmol/L KCl, 5 mmol/L MgCl₂, 0.1 mmol/L EDTA, and 15 µg/mL BSA) at 30 °C for 20 min in the presence of the indicated drug concentrations. Reactions were terminated by adding SDS (0.5% final concentration) followed by the addition of two volumes of loading dye (80% formamide, 10 mmol/L sodium hydroxide, 1 mmol/L sodium EDTA, 0.1% xylene cyanol, and 0.1% bromophenol blue). Aliquots of reaction mixtures were subjected to 20% denaturing PAGE. Gels were dried and visualised by using PhosphorImager and Image Quant software (Molecular Dynamics).

4.4. Kinases inhibitory assay

The IC₅₀ values of the tested compounds, Gefitinib and TAE226 on different nine kinases (EGFR, FAK, FRK, IGF-1R, BTK, c-Src, VEGFR-1, VEGFR-2, HER-2) were estimated utilising Z-LYTE® technology, which is based on FRET (Invitrogen/Life Technologies).

4.5. In silico molecular docking

Ligands were converted to 3D structures and minimised using Avogadro⁴⁸. Ligands were prepared and converted to pdbqt files using PyRx⁴⁹. Protein targets were downloaded from the protein data bank under the codes 1M17 for EGFR and 2JKM for FAK⁵⁰. Co-crystallised ligands were extracted from pdb files and prepared similar to the tested ligands. Docking was done using Autodock Vina⁵¹ in a grid box of 25³ Å³ centred on the co-crystallised ligand with exhaustiveness of 16. Visualisation and 3D images were prepared using PyMol⁵².

4.6. Molecular dynamics (MD) simulation

Missing loops in the 3D structures of the protein were constructed using Swiss-Model⁴³ before starting molecular dynamics steps. All atom molecular dynamics simulations were performed using GROMACS 2020.3⁵³ for the selected protein-ligand complexes as reported earlier⁵⁴. In brief, SwissParam server⁵⁵ was used for ligands parameterisation while Charmm36 all-atom force field⁵⁶ was used to generate topology files for the protein. Ligand coordinates obtained from docking studies were used to build complexes which were boxed in a dodecahedron box and then solvated with TIP3P⁵⁷ explicit water. Systems were neutralised by the addition of required number of Na⁺ or Cl⁻ ions. Systems energy was minimised with a maximum force of 1000 kJ mol⁻¹ nm⁻¹ using steepest descent algorithm. Equilibration using NVT and NPT ensembles for 1 ns each was done afterward then production run was done for 50 ns. Temperature was kept at 300K using the V-rescale algorithm⁵⁸ while pressure was controlled using the Parrinello-Rahman barostat⁵⁹ as required. The LINear Constraint Solver (LINCS) algorithm⁶⁰ and Particle mesh Ewald (PME) method⁶¹ were used for bond's length constraints and long-range electrostatics calculations, respectively. Two femto-second timestep was used for all simulations. Van der Waals distance cut-off (rvdw) was set to 1.2 nm. Trajectories from the production run were used for analysis using trajconv after correction of periodic boundary condition (PBC).

Disclosure statement

The authors have declared no conflict of interest.

Funding

The authors acknowledge financial support from the Researchers Supporting Project number (RSP-2021/103), King Saud University, Riyadh, Saudi Arabia. Mostafa M. Elbadawi has been supported by MEXT scholarship provided by the Ministry of Education, Culture, Sports, Science and Technology of Japan (scholarship no. 182582). Also, Yves Pommier and Keli K. Agama have been supported by the Center for Cancer Research, the Intramural Program of the National Cancer Institute, NIH (BC-006161). Moreover, Amer Ali Abd El-Hafeez was supported by an NIH-funded Cancer Therapeutics Training Program (CT2, T32 CA121938) and Pradipta Ghosh was supported by the NIH (CA238042, CA100768, and CA160911).

References

- Peng CK, Zeng T, Xu XJ, et al. Novel 4-(4-substituted amido-benzyl)furan-2(5H)-one derivatives as topoisomerase I inhibitors. *Eur J Med Chem* 2017;127:187–99.
- Mohassab AM, Hassan HA, Abdelhamid D, et al. Design and synthesis of novel quinoline/chalcone/1,2,4-triazole hybrids as potent antiproliferative agent targeting EGFR and BRAFV600E kinases. *Bioorg Chem* 2021;106:104510.
- Kovvuri J, Nagaraju B, Nayak VL, et al. Design, synthesis and biological evaluation of new β-carboline-bisindole compounds as DNA binding, photocleavage agents and topoisomerase I inhibitors. *Eur J Med Chem* 2018;143:1563–77.
- Sung H, Ferlay J, Siegel RL, et al. Global cancer statistics 2020: GLOBOCAN estimates of incidence and mortality worldwide for 36 cancers in 185 countries. *CA Cancer J Clin* 2021;71:209–49.
- Khodair AI, Elbadawi MM, Elsaady MT, Abdellatif KRA. Design, synthesis, molecular docking and cytotoxicity evaluation of some novel 5-arylidene-3-(substituted phenyl)-2-(p-tolylamino)-4-imidazolones. *J Appl Pharm Sci* 2017;7:58–68.
- Bray F, Ferlay J, Soerjomataram I, et al. Global cancer statistics 2018: GLOBOCAN estimates of incidence and mortality worldwide for 36 cancers in 185 countries. *CA Cancer J Clin* 2018;68:394–424.
- Xie H, Lin X, Zhang Y, et al. Design, synthesis and biological evaluation of ring-fused pyrazoloamino pyridine/pyrimidine derivatives as potential FAK inhibitors. *Bioorganic Med Chem Lett* 2020;30:127459.
- Elbadawi MM, Eldehna WM, Nocentini A, et al. Identification of N-phenyl-2-(phenylsulfonyl)acetamides/propanamides as new SLC-0111 analogues: synthesis and evaluation of the carbonic anhydrase inhibitory activities. *Eur J Med Chem* 2021;218:113360.
- Abdellatif KRA, Elbadawi MM, Elsaady MT, et al. Design, synthesis and cytotoxicity evaluation of new 3, 5-disubstituted-2-thioxoimidazolidinones. *Anticancer Agents Med Chem* 2018;18:573–82.
- Ismail RSM, Abou-Seri SM, Eldehna WM, et al. Novel series of 6-(2-substitutedacetamido)-4-anilinoquinazolines as EGFR-ERK signal transduction inhibitors in MCF-7 breast cancer cells. *Eur J Med Chem* 2018;155:782–96.

11. Wang Z, Wu X, Wang L, et al. Facile and efficient synthesis and biological evaluation of 4-anilinoquinazoline derivatives as EGFR inhibitors. *Bioorg Med Chem Lett* 2016;26:2589–93.
12. Hu S, Xie G, Zhang DX, et al. Synthesis and biological evaluation of crown ether fused quinazoline analogues as potent EGFR inhibitors. *Bioorg Med Chem Lett* 2012;22:6301–5.
13. Dawson JC, Serrels A, Stupack DG, et al. Targeting FAK in anticancer combination therapies. *Nat Rev Cancer* 2021;21:313–24.
14. Dao P, Jarray R, Coq JL, et al. Synthesis of novel diarylamino-1,3,5-triazine derivatives as FAK inhibitors with anti-angiogenic activity. *Bioorg Med Chem Lett* 2013;23:4552–6.
15. Wang R, Zhao X, Yu S, et al. Discovery of 7*H*-pyrrolo[2,3-*d*]pyridine derivatives as potent FAK inhibitors: design, synthesis, biological evaluation and molecular docking study. *Bioorg Chem* 2020;102:104092.
16. Li B, Li Y, Tomkiewicz-Raulet C, et al. Design, synthesis, and biological evaluation of covalent inhibitors of focal adhesion kinase (FAK) against human malignant glioblastoma. *J Med Chem* 2020;63:12707–24.
17. Gavriil ES, Doukatas A, Karampelas T, et al. Design, synthesis and biological evaluation of novel substituted purine isomers as EGFR kinase inhibitors, with promising pharmacokinetic profile and *in vivo* efficacy. *Eur J Med Chem* 2019;176:393–409.
18. McLean GW, Carragher NO, Avizienyte E, et al. The role of focal-adhesion kinase in cancer – a new therapeutic opportunity. *Nat Rev Cancer* 2005;5:505–15.
19. Luo QY, Zhou SN, Pan WT, et al. A multi-kinase inhibitor APG-2449 enhances the antitumor effect of ibrutinib in esophageal squamous cell carcinoma via EGFR/FAK pathway inhibition. *Biochem Pharmacol* 2021;183:114318.
20. Ai M, Wang C, Tang Z, et al. Design and synthesis of diphenylpyrimidine derivatives (DPPYs) as potential dual EGFR T790M and FAK inhibitors against a diverse range of cancer cell lines. *Bioorg Chem* 2020;94:103408.
21. Eke I, Cordes N. Dual targeting of EGFR and focal adhesion kinase in 3D grown HNSCC cell cultures. *Radiother Oncol* 2011;99:279–86.
22. Yadav P, Shah K. Quinolines, a perpetual, multipurpose scaffold in medicinal chemistry. *Bioorg Chem* 2021;109:104639.
23. Karnik KS, Sarkate AP, Tiwari SV, et al. Computational and synthetic approach with biological evaluation of substituted quinoline derivatives as small molecule L858R/T790M/C797S triple mutant EGFR inhibitors targeting resistance in non-small cell lung cancer (NSCLC). *Bioorg Chem* 2021;107:104612.
24. Matada BS, Pattanashettar R, Yernale NG. A comprehensive review on the biological interest of quinoline and its derivatives. *Bioorg Med Chem* 2021;32:115973.
25. Weyesa A, Mulugeta E. Recent advances in the synthesis of biologically and pharmaceutically active quinoline and its analogues: a review. *RSC Adv* 2020;10:20784–93.
26. Afzal O, Kumar S, Haider MR, et al. A review on anticancer potential of bioactive heterocycle quinoline. *Eur J Med Chem* 2015;97:871–910.
27. Wu P, Nielsen TE, Clausen MH. FDA-approved small-molecule kinase inhibitors. *Trends Pharmacol Sci* 2015;36:422–39.
28. He R, Xu B, Ping L, Lv X. Structural optimization towards promising β -methyl-4-acrylamido quinoline derivatives as PI3K/mTOR dual inhibitors for anti-cancer therapy: The *in vitro* and *in vivo* biological evaluation. *Eur J Med Chem* 2021;214:113249.
29. Nan X, Li HJ, Fang SB, et al. Structure-based discovery of novel 4-(2-fluorophenoxy)quinoline derivatives as c-Met inhibitors using isocyanide-involved multicomponent reactions. *Eur J Med Chem* 2020;193:112241.
30. Li K, Li Y, Zhou D, et al. Synthesis and biological evaluation of quinoline derivatives as potential anti-prostate cancer agents and Pim-1 kinase inhibitors. *Bioorg Med Chem* 2016;24:1889–97.
31. Pannala M, Kher S, Wilson N, et al. Synthesis and structure-activity relationship of 4-(2-aryl-cyclopropylamino)-quinoline-3-carbonitriles as EGFR tyrosine kinase inhibitors. *Bioorg Med Chem Lett* 2007;17:5978–82.
32. Pawar VG, Sos ML, Rode HB, et al. Synthesis and biological evaluation of 4-anilinoquinolines as potent inhibitors of epidermal growth factor receptor. *J Med Chem* 2010;53:2892–901.
33. Li S, Hu L, Li J, et al. Design, synthesis, structure-activity relationships and mechanism of action of new quinoline derivatives as potential antitumor agents. *Eur J Med Chem* 2019;162:666–78.
34. Abouzid K, Shouman S. Design, synthesis and *in vitro* antitumor activity of 4-aminoquinoline and 4-aminoquinazoline derivatives targeting EGFR tyrosine kinase. *Bioorg Med Chem* 2008;16:7543–51.
35. Tsou HR, Overbeek-Klumpers EG, Hallett WA, et al. Optimization of 6,7-disubstituted-4-(arylamino)quinoline-3-carbonitriles as orally active, irreversible inhibitors of human epidermal growth factor receptor-2 kinase activity. *J Med Chem* 2005;48:1107–31.
36. Elbadawi MM, Eldehna WM, Wang W, et al. Discovery of 4-alkoxy-2-aryl-6,7-dimethoxyquinolines as a new class of topoisomerase I inhibitors endowed with potent *in vitro* anticancer activity. *Eur J Med Chem* 2021;215:113261.
37. Pommier Y. Drugging topoisomerases: lessons and challenges. *ACS Chem Biol* 2013;8:82–95.
38. Marzi L, Agama K, Murai J, et al. Novel fluoroindenoisoquinoline non-camptothecin topoisomerase I inhibitors. *Mol Cancer Ther* 2018;17:1694–704.
39. Dexheimer TS, Pommier Y. DNA cleavage assay for the identification of topoisomerase I inhibitors. *Nat Protoc* 2008;3:1736–50.
40. Antony S, Jayaraman M, Laco G, et al. Differential induction of topoisomerase I-DNA cleavage complexes by the indenoisoquinoline MJ-III-65 (NSC 706744) and camptothecin: base sequence analysis and activity against camptothecin-resistant topoisomerases I. *Cancer Res* 2003;63:7428–35.
41. Elsayed MSA, Su Y, Wang P, et al. Design and synthesis of chlorinated and fluorinated 7-azaindenoisoquinolines as potent cytotoxic anticancer agents that inhibit topoisomerase I. *J Med Chem* 2017;60:5364–76.
42. Bell EW, Zhang Y. DockRMSD: an open-source tool for atom mapping and RMSD calculation of symmetric molecules through graph isomorphism. *J Cheminform* 2019;11:1–9.
43. Waterhouse A, Bertoni M, Bienert S, et al. SWISS-MODEL: homology modelling of protein structures and complexes. *Nucleic Acids Res* 2018;46:W296–303.
44. Zhao S, hong He Y, Wu D, Guan Z. A new general approach to 4-substituted-3-halo-2-quinolones. *J Fluor Chem* 2010;131:597–605.

45. Butin AV, Smirnov SK, Stroganova TA, et al. Simple route to 3-(2-indolyl)-1-propanones via a furan recyclization reaction. *Tetrahedron* 2007;63:474–91.
46. Huang Z, Yang Y, Xiao Q, et al. Auto-tandem catalysis: synthesis of acridines by Pd-catalyzed C=C bond formation and C(sp²)-N cross-coupling. *Eur J Org Chem* 2012;2012:6586–93.
47. Mamidala R, Subramani MS, Samsar S, et al. Chemoselective alkylation of aminoacetophenones with alcohols by using a palladacycle-phosphine catalyst. *Eur J Org Chem* 2018;2018: 6286–96.
48. Hanwell MD, Curtis DE, Lonie DC, et al. Avogadro: an advanced semantic chemical editor, visualization, and analysis platform. *J Cheminform* 2012;4:17.
49. Dallakyan S, Olson AJ. Small-molecule library screening by docking with PyRx. *Methods Mol Biol* 2015;1263:243–50.
50. Protein data bank, n.d. Available from: <https://www.rcsb.org/>
51. Trott O, Olson AJ. Software news and update AutoDock Vina: improving the speed and accuracy of docking with a new scoring function, efficient optimization, and multi-threading. *J Comput Chem* 2010;31:455–61.
52. The PyMOL molecular graphics system, n.d.
53. Abraham MJ, Murtola T, Schulz R, et al. Gromacs: high performance molecular simulations through multi-level parallelism from laptops to supercomputers. *SoftwareX* 2015;1–2: 19–25.
54. Said MA, Albohy A, Abdelrahman MA, Ibrahim HS. Importance of glutamine 189 flexibility in SARS-CoV-2 main protease: lesson learned from *in silico* virtual screening of ChEMBL database and molecular dynamics. *Eur J Pharm Sci* 2021;160:105744.
55. Zoete V, Cuendet MA, Grosdidier A, Michielin O. SwissParam: a fast force field generation tool for small organic molecules. *J Comput Chem* 2011;32:2359–68.
56. Huang J, Mackerell AD. CHARMM36 all-atom additive protein force field: validation based on comparison to NMR data. *J Comput Chem* 2013;34:2135–45.
57. Mark P, Nilsson L. Structure and dynamics of the TIP3P, SPC, and SPC/E water models at 298 K. *J Phys Chem A* 2001;105: 9954–60.
58. Bussi G, Donadio D, Parrinello M. Canonical sampling through velocity rescaling. *J Chem Phys* 2007;126:014101.
59. Parrinello M, Rahman A. Polymorphic transitions in single crystals: a new molecular dynamics method. *J Appl Phys* 1981;52:7182–90.
60. Hess B, Bekker H, Berendsen HJC, Fraaije JGEM. LINCS: a linear constraint solver for molecular simulations. *J Comput Chem* 1997;18:1463–72.
61. Darden T, York D, Pedersen L. Particle mesh Ewald: An N·log(N) method for Ewald sums in large systems. *J Chem Phys* 1993;98:10089–92.